

Quadratic Gating Functions in Mixture of Experts: A Statistical Insight

Pedram Akbarian^{†,*} Huy Nguyen^{†,*} Xing Han^{‡,*} Nhat Ho[†]

The University of Texas at Austin[†]

Johns Hopkins University[‡]

October 16, 2024

Abstract

Mixture of Experts (MoE) models are highly effective in scaling model capacity while preserving computational efficiency, with the gating network, or router, playing a central role by directing inputs to the appropriate experts. In this paper, we establish a novel connection between MoE frameworks and attention mechanisms, demonstrating how quadratic gating can serve as a more expressive and efficient alternative. Motivated by this insight, we explore the implementation of quadratic gating within MoE models, identifying a connection between the self-attention mechanism and the quadratic gating. We conduct a comprehensive theoretical analysis of the quadratic softmax gating MoE framework, showing improved sample efficiency in expert and parameter estimation. Our analysis provides key insights into optimal designs for quadratic gating and expert functions, further elucidating the principles behind widely used attention mechanisms. Through extensive evaluations, we demonstrate that the quadratic gating MoE outperforms the traditional linear gating MoE. Moreover, our theoretical insights have guided the development of a novel attention mechanism, which we validated through extensive experiments. The results demonstrate its favorable performance over conventional models across various tasks.

1 Introduction

The mixture of experts (MoE) [15, 17] architecture has recently become a powerful approach in conditional computation, driving many advances in machine learning. Unlike dense models, MoEs dynamically activates only a subset of network, known as “expert”, for each input. This results in an efficient form of conditional computation. A notable modern example is the sparsely gated MoE [36], which significantly increases the model capacity without a corresponding increase in computational costs [19, 10, 11]. This has made MoEs crucial for scaling up large language [16, 30, 42, 8], vision [32, 20, 33], and multimodal models [24, 12], resulting in outstanding performance in different areas.

The mixture of experts (MoE) model includes N expert networks and a gating network. Each expert $\mathbf{h}_i(\cdot; \boldsymbol{\eta}_i)$ transforms the input $\mathbf{x} \in \mathbb{R}^d$ into an output in \mathbb{R}^{d_o} . The gating network computes the gating probabilities $\mathbf{g}(\mathbf{x}; \boldsymbol{\Theta}_g) = (g_1(\mathbf{x}; \boldsymbol{\Theta}_g), \dots, g_N(\mathbf{x}; \boldsymbol{\Theta}_g))$, with $\boldsymbol{\Theta}_g$ as learnable parameters. The model output \mathbf{y} is the weighted sum of expert outputs: $\mathbf{y} = \sum_{i=1}^N g_i(\mathbf{x}; \boldsymbol{\Theta}_g) \cdot \mathbf{h}_i(\mathbf{x}; \boldsymbol{\eta}_i)$. In the original MoE framework [15, 17], the gating network \mathbf{g} computes scores for each expert using a

* Equal contribution.

parameterized network $\mathbf{s}(\mathbf{x}; \Theta_g) = (s_1(\mathbf{x}; \Theta_1), \dots, s_N(\mathbf{x}; \Theta_N)) \in \mathbb{R}^N$ and uses a softmax function to normalize these scores into a gating probability vector. Consequently, the scalar $g_i(\mathbf{x}; \Theta_g)$ can be expressed as

$$g_i(\mathbf{x}; \Theta_g) = \frac{\exp(s_i(\mathbf{x}; \Theta_g))}{\sum_{j=1}^N \exp(s_j(\mathbf{x}; \Theta_g))}, \quad i = 1, \dots, N. \quad (1)$$

The scoring network typically utilizes a *linear* mapping, which has been consistently adopted in modern sparse MoEs [36, 19, 10, 16, 6] due to its simplicity and scalability.

In this paper, we initially establish a connection between the MoE framework and the attention mechanism. In particular, we discuss that both MoE models and attention mechanisms aim to allocate computational resources efficiently by prioritizing relevant aspects of the input data. MoE models achieve this by using a gating network to selectively activate specialized experts, while the attention mechanism computes attention weights to emphasize important tokens or features in context. A detailed discussion is provided in Section 2.3. Additionally, we argue that the self-attention mechanism [39] assesses the interactions between different parts of the input to assign attention weights, which can be linked to the use of a quadratic scoring function in the gating network.

Inspired by this connection, we consider a class of *quadratic* gating MoE [21] models as an alternative to the conventional linear gating model. By allowing for more flexible decision boundaries through a quadratic scoring function, these models aim to provide better adaptability in expert selection. We particularly focus on two quadratic gatings: (1) *Quadratic polynomial gating*, which is inspired by the linear embeddings with biases of keys and queries in the attention (see Section 2.3) and given by:

$$g_i(\mathbf{x}; \Theta_g) = \frac{\exp(\mathbf{x}^\top \mathbf{A}_i \mathbf{x} + \mathbf{b}_i^\top \mathbf{x} + c_i)}{\sum_{j=1}^N \exp(\mathbf{x}^\top \mathbf{A}_j \mathbf{x} + \mathbf{b}_j^\top \mathbf{x} + c_j)}, \quad (2)$$

where $\Theta_g = \{(\mathbf{A}_i, \mathbf{b}_i, c_i) \in \mathbb{R}^{d \times d} \times \mathbb{R}^d \times \mathbb{R}, i = 1, \dots, N\}$ is the set of learnable parameters; (2) *Quadratic monomial gating*, which is motivated by the widely used linear embeddings without biases of keys and queries in the attention (see Section 2.3) and given by:

$$g_i(\mathbf{x}; \Theta_g) = \frac{\exp(\mathbf{x}^\top \mathbf{A}_i \mathbf{x} + c_i)}{\sum_{j=1}^N \exp(\mathbf{x}^\top \mathbf{A}_j \mathbf{x} + c_j)}, \quad (3)$$

where $\Theta_g = \{(\mathbf{A}_i, c_i) \in \mathbb{R}^{d \times d} \times \mathbb{R}, i = 1, \dots, N\}$ is the set of learnable parameters. In Appendix A, we further provided related literature on these choices of quadratic gatings.

Table 1: Summary of parameter estimation rates under the mixture of strongly identifiable experts models equipped with the quadratic polynomial gate and the quadratic monomial gate.

| Gate | Loss | $\exp(c_j^*)$ | \mathbf{A}_j^* | \mathbf{b}_j^* | $\boldsymbol{\eta}_j^*$ |
|---------------------------------|-----------------|-----------------------------------|--|---|-----------------------------------|
| Quadratic Polynomial (Thm. 3.3) | \mathcal{L}_1 | $\tilde{\mathcal{O}}_P(n^{-1/2})$ | $\tilde{\mathcal{O}}_P(n^{-1/\bar{r}(\mathcal{A}_j)})$ | $\tilde{\mathcal{O}}_P(n^{-1/2\bar{r}(\mathcal{A}_j)})$ | $\tilde{\mathcal{O}}_P(n^{-1/4})$ |
| Quadratic Monomial (Thm. B.3) | \mathcal{L}_3 | $\tilde{\mathcal{O}}_P(n^{-1/2})$ | $\tilde{\mathcal{O}}_P(n^{-1/4})$ | $\tilde{\mathcal{O}}_P(n^{-1/4})$ | $\tilde{\mathcal{O}}_P(n^{-1/4})$ |

Contributions. The paper has three main contributions, which can be summarized as follows:

1. Connection between attention mechanism and quadratic gating MoE. We begin by rigorously defining the MoE framework and the attention mechanism, highlighting the similarity in their formulations (see Definitions 2.1 and 2.2). Building on the similarity in their formulations, we unify these two popular concepts by introducing the Attention Gating Mixture of Experts framework (see Definition 2.3). This framework specifically highlights that the MoE framework can be effectively formulated as an attention mechanism. In particular, we connect the concepts of *query*, *keys*, and *values* from the attention mechanism to the MoE framework, creating a cohesive and robust unified model. We further demonstrate that the quadratic gating MoE is intrinsically linked to the self-attention mechanism, illustrating that it can be viewed as a special case within this unified framework (see Equation 8). This connection motivates us to study the quadratic gating MoE in more detail.

2. Theoretical analysis of the quadratic gating MoE. We explore the effects of two variants of the quadratic gating, namely the quadratic polynomial gating and the quadratic monomial gating, on the convergence of parameter and expert estimation under the MoE models. For the convergence analysis of each gate, we provide a corresponding strong identifiability condition (see Definitions 3.2 and B.2) to characterize the compatible structure of experts with that gate. Based on those conditions, we show that experts formulated as neural networks with activation functions such as ReLU and tanh require fewer data to approximate than linear experts (see Theorems 3.3 and C.1).

3. Practical implications. The convergence analysis of the quadratic gating MoE models provides two practical implications. Firstly, they show the benefits of quadratic monomial gating over quadratic polynomial gating, which confirms the benefits of the widely used linear embeddings of the keys and queries without bias terms in the attention mechanism in practice. Secondly, the theoretical analysis encourages the usage of non-linear experts over linear experts in quadratic gating MoE models. Given that insight, we propose a novel *active-attention mechanism* in equation (20) by replacing the linear value matrix by the non-linear value matrix in the attention mechanism. Through extensive empirical evaluation, we show the favorable performance of the proposed active-attention over standard attention in various tasks.

Organization. The paper proceeds as follows. In Section 2, we provide background on MoE layer, attention mechanism and their connection. Next, we investigate the convergence behavior of parameter and expert estimation under the MoE model with two variants of the quadratic gate, and present two important practical implications from that analysis in Section 3. Subsequently, we conduct extensive experiments to empirically justify the theoretical results and favorable performance of the active-attention mechanism. Finally, we conclude the paper in Section 6. Full proofs and the remaining materials are deferred to the Appendices.

Notations. We let $[n] := \{1, 2, \dots, n\}$ for any $n \in \mathbb{N}$. Next, for any set S , we denote $|S|$ as its cardinality. For any vector $\mathbf{v} \in \mathbb{R}^d$ and $\boldsymbol{\alpha} := (\alpha_1, \alpha_2, \dots, \alpha_d) \in \mathbb{N}^d$, we let $\mathbf{v}^{\boldsymbol{\alpha}} = v_1^{\alpha_1} v_2^{\alpha_2} \dots v_d^{\alpha_d}$, $|\mathbf{v}| := v_1 + v_2 + \dots + v_d$ and $\boldsymbol{\alpha}! := \alpha_1! \alpha_2! \dots \alpha_d!$, while $\|\mathbf{v}\|$ stands for its ℓ_2 -norm value. The probability simplex is denoted by $\Delta^{N-1} = \{\mathbf{x} \in \mathbb{R}^N : \sum_{i=1}^N x_i = 1, x_i \geq 0\}$. Lastly, for any two positive sequences $(a_n)_{n \geq 1}$ and $(b_n)_{n \geq 1}$, we write $a_n = \mathcal{O}(b_n)$ or $a_n \lesssim b_n$ if $a_n \leq Cb_n$ for all $n \in \mathbb{N}$, where $C > 0$ is some universal constant. The notation $a_n = \mathcal{O}_P(b_n)$ indicates that a_n/b_n is stochastically bounded, while $a_n = \tilde{\mathcal{O}}_P(b_n)$ means that the previous inequality occurs up to a logarithmic factor of n .

2 Background

In this section, we initially introduce the MoE layer and the attention mechanism in a formal manner. Following this, we investigate the connections between the MoE framework and the attention mechanism. Furthermore, leveraging these connections, we demonstrate how quadratic gating in MoE can be understood as a self-attention mechanism.

2.1 Mixture of Experts (MoE) Layer

The mixture of experts (MoE) layer includes N expert networks and a gating network. The gating network $\mathbf{g}(\cdot; \Theta_g)$ assigns input points to probability vectors, effectively partitioning the input space. It calculates a scoring function $\mathbf{s}(\cdot; \Theta_g)$ for each expert and normalizes these scores using $\sigma(\cdot)$ to form gating probabilities $\mathbf{g}(\mathbf{x}; \Theta_g) = \sigma(\mathbf{s}(\mathbf{x}; \Theta_g))$. Originally, dense MoE uses softmax for normalization [17], while sparse MoE uses Top- K softmax for sparsity [36]. Each score $s_i(\mathbf{x}; \Theta_g)$ links an input \mathbf{x} to an expert, and σ ensures that these scores sum to one. In this work, we assume that the scoring network can be written as $s_i(\mathbf{x}; \Theta_g) = s_g(\mathbf{x}; \theta_i)$ for all $i \in [N]$, where $s_g(\cdot; \theta): \mathbb{R}^d \rightarrow \mathbb{R}$ is a *gating scoring function*. Note that this assumption holds for all commonly used gating strategies. Here, we provide a formal definition of MoE layer:

Definition 2.1 (Mixture of Experts). Consider N parameterized experts $\mathbf{h}_i(\cdot; \eta_i): \mathbb{R}^d \rightarrow \mathbb{R}^{d_o}$ for $1 \leq i \leq N$, a parameterized scoring function $s_g(\cdot; \theta): \mathbb{R}^d \rightarrow \mathbb{R}$, and a normalization function $\sigma: \mathbb{R}^N \rightarrow \Delta^{N-1}$. Let $\Theta_g = (\theta_1^\top, \dots, \theta_N^\top)$ and $\Theta_e = (\eta_1^\top, \dots, \eta_N^\top)$ be the set of learnable parameters for the gating network and the experts, respectively. The MoE layer is defined by

$$\text{MoE}(\mathbf{x}; \Theta_g, \Theta_e) := \sum_{i=1}^N g_i(\mathbf{x}; \Theta_g) \cdot \mathbf{h}_i(\mathbf{x}; \eta_i), \quad (4)$$

where gating function is given by $\mathbf{g}(\mathbf{x}; \Theta_g) := \sigma(s_g(\mathbf{x}; \theta_1), \dots, s_g(\mathbf{x}; \theta_N))$.

2.2 Attention Mechanism

The attention mechanism [2, 39] enables transformers to focus dynamically on various parts of an input sequence, capturing essential dependencies and context. The formal definition of the attention mechanism is presented below:

Definition 2.2 (Attention Mechanism). Consider a *key* matrix $\mathbf{K} = (\mathbf{k}_1^\top, \dots, \mathbf{k}_N^\top) \in \mathbb{R}^{N \times d}$ that contains N key vectors and a *value* matrix $\mathbf{V} = (\mathbf{v}_1^\top, \dots, \mathbf{v}_N^\top) \in \mathbb{R}^{N \times d_v}$ that includes the corresponding N value vectors. We also define $s_\alpha: \mathbb{R}^d \times \mathbb{R}^d \rightarrow \mathbb{R}$ as an *attention scoring function* and $\sigma: \mathbb{R}^N \rightarrow \Delta^{N-1}$ as a normalization function. Given a *query* vector, $\mathbf{q} \in \mathbb{R}^d$, *Attention* on (\mathbf{K}, \mathbf{V}) is defined as

$$\text{Att}(\mathbf{q}, \mathbf{K}, \mathbf{V}) := \sum_{i=1}^N \alpha_i(\mathbf{q}, \mathbf{K}) \cdot \mathbf{v}_i, \quad (5)$$

where attention weights are defined as $\alpha(\mathbf{q}, \mathbf{K}) := \sigma(s_\alpha(\mathbf{q}, \mathbf{k}_1), \dots, s_\alpha(\mathbf{q}, \mathbf{k}_N))$.

The attention mechanism often uses the scaled dot product $s_\alpha(\mathbf{q}, \mathbf{k}) = \langle \mathbf{q}, \mathbf{k} \rangle / \sqrt{d}$ for the scoring function and normalizes using softmax, simplifying to $\text{Att}(\mathbf{q}, \mathbf{K}, \mathbf{V}) = \text{Softmax}\left(\frac{\mathbf{q}^\top \mathbf{K}^\top}{\sqrt{d}}\right) \mathbf{V}$.

2.3 Mixture of Experts as an Attention

MoE models integrate attention by dynamically routing inputs to various experts via a learned gating function. The recent MoEAtt model [3] uses an attention-based routing gate to further explore the link between attention mechanisms and MoE frameworks.

The MoEAtt model functions as an attention mechanism with the query vector as the input \mathbf{x} , the i th key vector as the *hidden representation* of the i th expert for \mathbf{x} , and the value vectors as the outputs of the expert networks. Building on the similarity in the formulation of MoE and attention mechanisms, we now extend the MoEAtt framework to incorporate a more generalized attention-based gating mechanism:

Definition 2.3 (Attention Gating Mixture of Experts). Extending Definition 2.1, consider parameterized query and key functions denoted by $\mathbf{q}(\cdot; \Theta^q): \mathbb{R}^d \rightarrow \mathbb{R}^d$ and $\mathbf{k}(\cdot; \Theta_i^k): \mathbb{R}^d \rightarrow \mathbb{R}^d$, respectively, and let s_α be an attention scoring function. Then, *Attention Gating Mixture of Experts* is achieved by employing the following gating scoring function:

$$s_g(\mathbf{x}; \Theta^q, \Theta_i^k) = s_\alpha(\mathbf{q}(\mathbf{x}; \Theta^q), \mathbf{k}(\mathbf{x}; \Theta_i^k)), \quad (6)$$

where $\Theta_g = \{(\Theta^q, \Theta_i^k), 1 \leq i \leq N\}$ is the set of learnable gating parameters. Specifically, the output of the Attention Gating MoE can be written as

$$\text{Att-MoE}(\mathbf{x}; \Theta_g, \Theta_e) := \text{Att}(\mathbf{q}(\mathbf{x}; \Theta^q), \mathbf{K}(\mathbf{x}; \Theta^k), \mathbf{V}(\mathbf{x}; \Theta_e)), \quad (7)$$

where $\mathbf{k}(\cdot; \Theta_i^k)$ represents the i th row of the key matrix $\mathbf{K}(\mathbf{x}; \Theta^k)$, and $\mathbf{h}_i(\mathbf{x}; \Theta_e)$ represents the i th row of the value matrix $\mathbf{V}(\mathbf{x}; \Theta_e)$ with Θ_e be the set of experts parameters.

In particular, the self-attention mechanism uses linear query and key functions along with a dot-product scoring function. This setting in Definition 2.3 leads to the formulation of a quadratic polynomial gating (2):

$$g_i(\mathbf{x}; \Theta_g) = \frac{\exp((\mathbf{W}^q \mathbf{x} + \mathbf{b}^q)^\top (\mathbf{W}_i^k \mathbf{x} + \mathbf{b}_i^k))}{\sum_{j=1}^N \exp((\mathbf{W}^q \mathbf{x} + \mathbf{b}^q)^\top (\mathbf{W}_j^k \mathbf{x} + \mathbf{b}_j^k))}, \quad (8)$$

where $\Theta_g = \{(\mathbf{W}^q, \mathbf{b}^q, \mathbf{W}_i^k, \mathbf{b}_i^k), 1 \leq i \leq N\}$ denotes the collection of gating parameters. It is noteworthy that in the implementation of the self-attention mechanism, often the bias terms are omitted. Here, we can adopt this in our formulation to obtain a quadratic monomial gating MoE (3):

$$g_i(\mathbf{x}; \Theta_g) = \frac{\exp(\mathbf{x}^\top \mathbf{W}^{q\top} \mathbf{W}_i^k \mathbf{x})}{\sum_{j=1}^N \exp(\mathbf{x}^\top \mathbf{W}^{q\top} \mathbf{W}_j^k \mathbf{x})}. \quad (9)$$

It should be noted that commonly used gating strategies can also be seamlessly expressed as an attention gating MoE. For instance, using an identity map as the query function and a constant key function with respect to the input \mathbf{x} restores the formulation to the traditional linear gating MoE.

Parameter count overhead. Introducing quadratic gating significantly increases the number of model parameters due to the additional quadratic terms in the gating network, which can lead to higher computational and memory demands. To mitigate this overhead, we can employ low-rank embeddings for the quadratic terms. Specifically, setting the query and key matrices \mathbf{W}^q and \mathbf{W}_i^k to dimensions $r \times d$ with $r \ll d$, we substantially reduce the number of additional parameters. This approach retains the advantages of quadratic gating while minimizing the overhead, making it a practical enhancement for MoE models. Appendix G offers a more thorough discussion on this topic.

3 Theoretical analysis of quadratic gating MoE

Motivated by the connection of quadratic MoE to attention in Section 2.3, we study the impacts of two variants of the quadratic gating on the convergence behavior of least squares expert estimation under a regression framework with the regression function taking the form of an MoE model. In particular, in Section 3.1, we examine a *quadratic polynomial gating* (2) in which the scoring function is a second-degree polynomial of the model input. Then, we investigate a *quadratic monomial gating* (3) where the scoring function is a second-degree monomial of the input in Appendix B. Furthermore, for the analysis of each quadratic gate, we derive an associated strong identifiability condition to determine which types of experts achieve better performance than others.

3.1 Quadratic Polynomial Gate

To begin with, let us formally present the regression framework used for our analysis of the quadratic polynomial gate. Assume that the data $(\mathbf{X}_1, Y_1), (\mathbf{X}_2, Y_2), \dots, (\mathbf{X}_n, Y_n) \in \mathbb{R}^d \times \mathbb{R}$ are i.i.d. sampled from the following model:

$$Y_i = f_{G_*}(\mathbf{X}_i) + \varepsilon_i, \quad i = 1, 2, \dots, n, \quad (10)$$

where $\varepsilon_1, \dots, \varepsilon_n$ are independent Gaussian noise variables such that $\mathbb{E}[\varepsilon_i | \mathbf{X}_i] = 0$ and $\text{Var}(\varepsilon_i | \mathbf{X}_i) = \sigma^2$ for all $1 \leq i \leq n$. Additionally, we assume that $\mathbf{X}_1, \mathbf{X}_2, \dots, \mathbf{X}_n$ are i.i.d. samples from some probability distribution μ . Above, the regression function $f_{G_*}(\cdot)$ admits the form of a quadratic polynomial gating MoE model with N^* experts, namely

$$f_{G_*}(\mathbf{x}) := \sum_{i=1}^{N^*} \frac{\exp(\mathbf{x}^\top \mathbf{A}_i^* \mathbf{x} + (\mathbf{b}_i^*)^\top \mathbf{x} + c_i^*)}{\sum_{j=1}^{N^*} \exp(\mathbf{x}^\top \mathbf{A}_j^* \mathbf{x} + (\mathbf{b}_j^*)^\top \mathbf{x} + c_j^*)} \cdot h(\mathbf{x}, \boldsymbol{\eta}_i^*), \quad (11)$$

where $(\mathbf{A}_i^*, \mathbf{b}_i^*, c_i^*, \boldsymbol{\eta}_i^*)_{i=1}^{N^*}$ are unknown ground-truth parameters in $\mathbb{R}^{d \times d} \times \mathbb{R}^d \times \mathbb{R} \times \mathbb{R}^q$, and $G_* := \sum_{i=1}^{N^*} \exp(c_i^*) \delta_{(\mathbf{A}_i^*, \mathbf{b}_i^*, \boldsymbol{\eta}_i^*)}$ denotes the associated *mixing measure*, a weighted sum of Dirac measures δ . Meanwhile, the function $h(\mathbf{x}; \boldsymbol{\eta})$ is referred to as the *expert function*, which we assumed to be of parametric form.

Least square estimation: To estimate the unknown parameters $(\mathbf{A}_i^*, \mathbf{b}_i^*, c_i^*, \boldsymbol{\eta}_i^*)_{i=1}^{N^*}$ or, equivalently, the ground-truth mixing measure G^* , we deploy the least squares estimator [38]:

$$\hat{G}_n := \arg \min_{G \in \mathcal{G}_N(\Theta)} \sum_{i=1}^n \left(y_i - f_G(\mathbf{x}_i) \right)^2, \quad (12)$$

where $\mathcal{G}_N(\Theta) := \{G = \sum_{i=1}^{N'} \exp(c_i) \delta_{(\mathbf{A}_i, \mathbf{b}_i, \boldsymbol{\eta}_i)} : 1 \leq N' \leq N, (\mathbf{A}_i, \mathbf{b}_i, c_i, \boldsymbol{\eta}_i) \in \Theta\}$ is the set of all mixing measures with at most N components, where $N > N^*$. The goal of this paper is to explore the convergence properties of the estimator \hat{G}_n in a fixed-dimensional setting.

Given the above least squares estimator, we demonstrate in Theorem 3.1 that the convergence rate of regression estimation is parametric on the sample size.

Theorem 3.1 (Regression Estimation Rate). *Equipped with a least squares estimator \hat{G}_n given in equation (12), the model estimation $f_{\hat{G}_n}$ converges to the true model f_{G_*} at the following rate:*

$$\|f_{\hat{G}_n} - f_{G_*}\|_{L_2(\mu)} = \tilde{\mathcal{O}}_P(n^{-1/2}). \quad (13)$$

Proof of Theorem 3.1 is in Appendix D.1. From the result of this theorem, it can be seen that if we are able to establish the lower bound $\|f_{\hat{G}_n} - f_{G_*}\|_{L_2(\mu)} \gtrsim \mathcal{L}(\hat{G}_n, G_*)$ where \mathcal{L} is some loss function among parameters, then we obtain the parameter estimation rate $\mathcal{L}(\hat{G}_n, G_*) = \tilde{\mathcal{O}}_P(n^{-1/2})$. This approach plays an vital role in establishing the rates for estimating individual parameters as well as experts in the sequel.

Turning to the parameter and expert estimation problem. A key step to establish the parameter and expert estimation rates is to decompose the discrepancy $f_{\hat{G}_n}(\mathbf{x}) - f_{G_*}(\mathbf{x})$ into a combination of linearly independent terms via Taylor expansions to the function $F(\mathbf{x}; \mathbf{A}, \mathbf{b}, \boldsymbol{\eta}) := \exp(\mathbf{x}^\top \mathbf{A} \mathbf{x} + \mathbf{b}^\top \mathbf{x}) h(\mathbf{x}, \boldsymbol{\eta})$. However, we notice that there is an interaction among gating parameters A and b expressed by the following partial differential equation (PDE):

$$\frac{\partial F}{\partial A}(\mathbf{x}; \mathbf{A}, \mathbf{b}, \boldsymbol{\eta}) = \frac{\partial^2 F}{\partial b \partial b^\top}(\mathbf{x}; \mathbf{A}, \mathbf{b}, \boldsymbol{\eta}). \quad (14)$$

Technically, such parameter interaction induces plenty of linearly dependent derivative terms in the decomposition of $f_{\hat{G}_n}(\mathbf{x}) - f_{G_*}(\mathbf{x})$, which is undesirable. To capture this interaction, we need to consider a system of polynomial equations as described below to construct a loss function among parameters used for the parameter estimation problem.

System of polynomial equations. Let $\bar{r}(m)$ be the smallest natural number r such that the following system of polynomial equations does not admit any non-trivial solutions for the unknown variables: $(p_l, \gamma_{1l}, \gamma_{2l})_{l=1}^m \subseteq \mathbb{R}^3$

$$\sum_{l=1}^m \sum_{\substack{n_1, n_2 \in \mathbb{N} \\ n_1 + 2n_2 = \alpha}} \frac{p_l^2 \gamma_{1l}^{n_1} \gamma_{2l}^{n_2}}{n_1! n_2!} = 0, \quad \alpha = 1, 2, \dots, r, \quad (15)$$

A solution to the above system is regarded as non-trivial if all variables p_l are non-zero, whereas at least one of the γ_{1l} is different from zero. As shown in [Proposition 2.1, [14]], we have $\bar{r}(2) = 4$, $\bar{r}(3) = 6$ and $\bar{r}(m) \geq 7$ when $m \geq 4$.

Next, we introduce a condition called *poly-strong identifiability* to characterize the types of expert functions that admit faster estimation rates than others. From a technical view, the purpose of the strong identifiability condition is to eliminate all potential interactions among expert parameters via some PDEs as in equation (14).

Definition 3.2 (Poly-strong identifiability). We say that an expert function $x \mapsto h(\mathbf{x}, \boldsymbol{\eta})$ is strongly identifiable if it is twice differentiable w.r.t its parameter $\boldsymbol{\eta}$, and if for any $k \geq 1$ and pair-wise different parameters $\boldsymbol{\eta}_1, \dots, \boldsymbol{\eta}_k$, the following set

$$\left\{ \mathbf{x}^\nu \cdot \frac{\partial^{|\gamma|} h}{\partial \boldsymbol{\eta}^\gamma}(\mathbf{x}; \boldsymbol{\eta}_j) : j \in [k], \nu \in \mathbb{N}^d, \gamma \in \mathbb{N}^q, 0 \leq |\gamma| \leq r_j, 0 \leq |\nu| \leq 2(r_j - |\gamma|) \right\},$$

is linearly independent for almost every \mathbf{x} for any $r_j \leq \bar{r}(N - N^* + 1)$.

Example. It can be verified that the poly-strong identifiability condition holds for experts formulated as feed-forward neural networks with activation functions such as $\text{ReLU}(\cdot)$ and $\tanh(\cdot)$. However, a linear expert fails to satisfy this condition.

In the sequel, we determine the parameter and expert estimation rates when using strongly identifiable experts and linear experts, respectively.

Poly-strongly identifiable experts. To capture the convergence behavior of strongly identifiable experts, let us construct a loss function among parameters based on a notion of Voronoi cells [22, 26, 25]. Given an arbitrary mixing measure G with $k' \leq k$ components, we distribute its components to the following Voronoi cells, which are generated by the components of G_* :

$$\mathcal{V}_j \equiv \mathcal{V}_j(G) := \{i \in [k'] : \|\omega_i - \omega_j^*\| \leq \|\omega_i - \omega_\ell^*\|, \forall \ell \neq j\}, \quad (16)$$

where $\omega_i := (\mathbf{A}_i, \mathbf{b}_i, \boldsymbol{\eta}_i)$ and $\omega_j^* := (\mathbf{A}_j^*, \mathbf{b}_j^*, \boldsymbol{\eta}_j^*)$ for any $j \in [N^*]$. Notably, the cardinality of Voronoi cell \mathcal{V}_j is exactly the number of fitted components that approximates ω_j^* . Then, the Voronoi loss function used for our analysis is given by:

$$\begin{aligned} \mathcal{L}_1(G, G_*) := & \sum_{j:|\mathcal{V}_j|>1} \sum_{i \in \mathcal{V}_j} \exp(c_i) \|\Delta\boldsymbol{\theta}_{ij}\|_{\frac{\bar{r}(|\mathcal{V}_j|)}{2}, \bar{r}(|\mathcal{V}_j|), 2} + \sum_{j:|\mathcal{V}_j|=1} \sum_{i \in \mathcal{V}_j} \exp(c_i) \|\Delta\boldsymbol{\theta}_{ij}\|_{1,1,1} \\ & + \sum_{j=1}^{N^*} \left| \sum_{i \in \mathcal{V}_j} \exp(c_i) - \exp(c_j^*) \right|, \end{aligned} \quad (17)$$

where we denote $\Delta\mathbf{A}_{ij} := \mathbf{A}_i - \mathbf{A}_j^*$, $\Delta\mathbf{b}_{ij} := \mathbf{b}_i - \mathbf{b}_j^*$, $\Delta\boldsymbol{\eta}_{ij} := \boldsymbol{\eta}_i - \boldsymbol{\eta}_j^*$, and $\Delta\boldsymbol{\theta}_{ij} = (\Delta\mathbf{A}_{ij}, \Delta\mathbf{b}_{ij}, \Delta\boldsymbol{\eta}_{ij})$. Furthermore, we define $\|\Delta\boldsymbol{\theta}_{ij}\|_{r_1, r_2, r_3} := \|\Delta\mathbf{A}_{ij}\|^{r_1} + \|\Delta\mathbf{b}_{ij}\|^{r_2} + \|\Delta\boldsymbol{\eta}_{ij}\|^{r_3}$ for any $r_1, r_2, r_3 \geq 1$.

Equipped with the Voronoi loss \mathcal{L}_1 defined above, we are now ready to capture the parameter estimation rate in Theorem 3.3, whose proof can be found in Appendix D.2.

Theorem 3.3. *Suppose that the expert function $h(\cdot, \boldsymbol{\eta})$ is strongly identifiable, then we achieve the following lower bound for any $G \in \mathcal{G}_k(\Theta)$:*

$$\|f_G - f_{G_*}\|_{L_2(\mu)} \gtrsim \mathcal{L}_1(G, G_*),$$

which together with Theorem 3.1 indicates that $\mathcal{L}_1(\widehat{G}_n, G_*) = \widetilde{\mathcal{O}}_P(n^{-1/2})$.

There are two main implications from the result of Theorem 3.3. First, it follows from the formulation of the loss function \mathcal{L}_1 that exact-specified parameters $\mathbf{A}_j^*, \mathbf{b}_j^*, \boldsymbol{\eta}_j^*$, i.e. $j \in [N^*] : |\mathcal{V}_j(\widehat{G}_n)| = 1$, share the same estimation rate of order $\widetilde{\mathcal{O}}_P(n^{-1/2})$. Note that as the expert $h(\cdot, \boldsymbol{\eta})$ is a Lipschitz function, then by denoting $\widehat{G}_n := \sum_{i=1}^{\widehat{k}_n} \exp(\widehat{c}_i^n) \delta_{(\widehat{\mathbf{A}}_i^n, \widehat{\mathbf{b}}_i^n, \widehat{\boldsymbol{\eta}}_i^n)}$, we get

$$\sup_x |h(\mathbf{x}, \widehat{\boldsymbol{\eta}}_i^n) - h(\mathbf{x}, \boldsymbol{\eta}_j^*)| \lesssim \|\widehat{\boldsymbol{\eta}}_i^n - \boldsymbol{\eta}_j^*\| = \widetilde{\mathcal{O}}_P(n^{-1/2}), \quad (18)$$

for any $i \in \mathcal{V}_j(\widehat{G}_n)$. The above bound indicates that if the strongly identifiable expert $h(\cdot, \boldsymbol{\eta}_j^*)$ is fitted by exactly one expert, it has an estimation rate is of order $\widetilde{\mathcal{O}}_P(n^{-1/2})$. Second, for over-specified parameters $\mathbf{A}_j^*, \mathbf{b}_j^*, \boldsymbol{\eta}_j^*$, where $j \in [N^*] : |\mathcal{V}_j(\widehat{G}_n)| > 1$, the rates for estimating them are substantially slower. In particular, the estimation rates for \mathbf{A}_j^* and \mathbf{b}_j^* are of orders $\widetilde{\mathcal{O}}_P(n^{-1/\bar{r}(|\mathcal{V}_j(\widehat{G}_n)|)})$ and $\widetilde{\mathcal{O}}_P(n^{-1/2\bar{r}(|\mathcal{V}_j(\widehat{G}_n)|)})$, respectively, which are determined by the solvability of the system (15). For instance, when those parameters are fitted by three components, the previous rates become $\widetilde{\mathcal{O}}_P(n^{-1/6})$ and $\widetilde{\mathcal{O}}_P(n^{-1/12})$. Meanwhile, parameters $\boldsymbol{\eta}_j^*$ enjoy an estimation rate of order $\widetilde{\mathcal{O}}_P(n^{-1/4})$. By arguing similarly to equation (18), the rates for estimating the experts $h(\cdot, \boldsymbol{\eta}_j^*)$ are also $\widetilde{\mathcal{O}}_P(n^{-1/4})$.

Poly-weak identifiability of linear experts. We note in passing that for linear expert function $h(\mathbf{x}, (\boldsymbol{\beta}_1, \beta_0)) = (\boldsymbol{\beta}_{1i})^\top \mathbf{x} + \beta_{0i}$, where $(\boldsymbol{\beta}_1, \beta_0) \in \mathbb{R}^d \times \mathbb{R}$, it violates the poly-strong identifiability condition due to an interaction among parameters via the following partial differential equation:

$$\frac{\partial^2 F}{\partial b \partial \beta_0}(\mathbf{x}; \mathbf{A}_i^*, \mathbf{b}_i^*, \boldsymbol{\beta}_{1i}^*, \beta_{0i}^*) = \frac{\partial F}{\partial \boldsymbol{\beta}_1}(\mathbf{x}; \mathbf{A}_i^*, \mathbf{b}_i^*, \boldsymbol{\beta}_{1i}^*, \beta_{0i}^*), \quad (19)$$

where we denote $F(\mathbf{x}; \mathbf{A}, \mathbf{b}, \boldsymbol{\beta}_1, \beta_0) := \exp(\mathbf{x}^\top \mathbf{A} \mathbf{x} + \mathbf{b}^\top \mathbf{x})(\boldsymbol{\beta}_1^\top \mathbf{x} + \beta_0)$. That violation leads to $\mathcal{O}(1/\log(n))$ rates of the parameters, which are considerably slower than those of strongly identifiable experts in Theorem 3.3. Please refer to Appendix C for a detailed argument of that result.

4 Practical Implications

In this section, we provide two practical implications from the convergence analysis of parameter and expert estimation under the MoE models with the quadratic polynomial gate in Section 3.1 and Appendix B.

1. Benefits of quadratic monomial gating (3) over quadratic polynomial gating (2). The remarks after Theorems 3.3 and B.3 indicate that the estimation rates of the gating parameters are independent of the amount of over-specification of the number of experts and much better than those of the polynomial gating parameters, which become very slow even when we only overspecify the model by a few experts. That theoretical advantage of the monomial gating over the polynomial gating confirms the benefits of the widely used linear embeddings of the keys and queries without bias terms in the attention in practice.

2. New attention mechanism. Both the poly-strong identifiability and mono-strong identifiability conditions shed light on the design of new attention mechanism in practice. In particular, we may avoid linear experts as these experts do not satisfy these identifiability conditions and lead to considerably slow rates of parameter and expert estimations. The linear experts correspond to the linear value matrix in the attention mechanism (5). The poly-strong identifiability and mono-strong identifiability conditions suggest the usage of non-linear experts, which corresponds to the following new attention mechanism:

$$\text{Act-Att}(\mathbf{q}, \mathbf{K}, \mathbf{V}) = \text{Softmax} \left(\frac{\mathbf{q}^\top \mathbf{K}^\top}{\sqrt{d}} \right) \bar{\sigma}(\mathbf{V}), \quad (20)$$

where $\bar{\sigma}(\cdot)$ is a non-linear function. We name the new attention mechanism (20) as *active-attention*. Our experiments with the active-attention in Figure 2 and Table 2 for both classification and time series forecasting tasks with a wide range of non-linear function $\bar{\sigma}(\cdot)$ demonstrate the favorable performance of active-attention over the standard attention mechanism.

5 Experiments

In this section, we conduct numerical experiments to verify the theoretical results presented in Section 3, the favorable performance of the proposed active-attention mechanism (20) over standard attention mechanism, and the empirical benefits of quadratic gating over standard linear gating in language modeling.

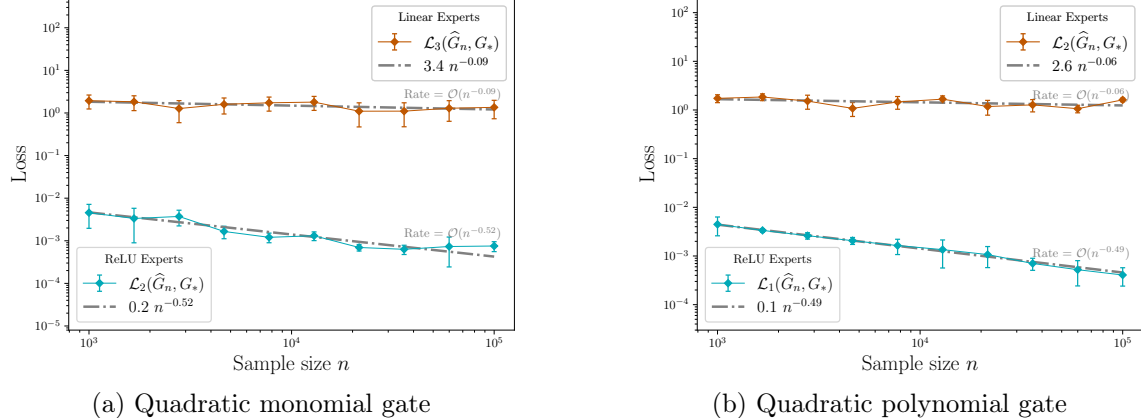


Figure 1: Logarithmic plots displaying empirical convergence rates. Subfigures 1a and 1b depict the empirical averages of the corresponding Voronoi losses for the quadratic polynomial and quadratic monomial settings, respectively. The orange lines and blue lines respectively depict the Voronoi loss associated with the linear experts and the ReLU experts. The gray dash-dotted lines are used to illustrate the fitted lines to indicate the empirical convergence rate.

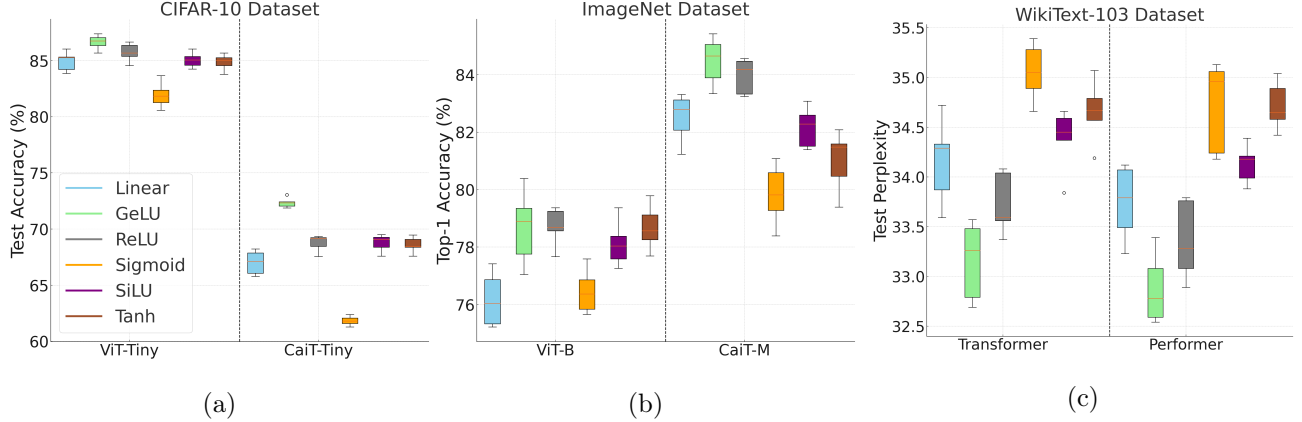


Figure 2: We evaluate the effect of employing five different nonlinear activation functions in the self-attention block and compare them with standard linear activation functions on (a) CIFAR-10, (b) ImageNet, and (c) WikiText-103 datasets. All results are averaged across five random experiments. The results demonstrate that using GELU and ReLU activation functions in various transformer backbones noticeably improves performance compared to the linear activation function.

Verification of theoretical results. We generate synthetic data based on the model described in equation (10). Details regarding the values of the true parameters and the training procedure can be found in the Appendix F.

We evaluate the empirical convergence rates of parameter estimation for (1) quadratic polynomial gate and (2) quadratic monomial gate involving linear and ReLU experts in an over-specified setting. Data for each experiment are produced following equation (10), based on the true model for each case. For each experiment, we compute the respective Voronoi losses for each model and present the average values for different sample sizes in Figure 1. Error bars representing two standard deviations are also shown. Figure 1a investigates the empirical convergence rates of linear and ReLU experts within a quadratic monomial gate setting.

Performance of active-attention mechanism. We empirically demonstrate the effects of

Table 2: We further assess the effectiveness of nonlinear activation functions on transformer-based time-series forecasting models across eight forecasting tasks. The results show the averaged mean squared error across five random experiments, with the best results highlighted in **bold** and the second-best results underlined. The results indicate that in most situations, Tanh and Sigmoid functions outperformed other activation functions in these tasks.

| Model \ Dataset | Weather | Traffic | Electricity | Illness | ETTh1 | ETTh2 | ETTm1 | ETTm2 | |
|-----------------|---------------|--------------|--------------|--------------|--------------|--------------|--------------|--------------|--------------|
| PatchTST | <i>Linear</i> | <i>0.197</i> | <i>0.383</i> | <i>0.152</i> | <i>1.474</i> | <i>0.414</i> | <i>0.338</i> | <i>0.331</i> | <i>0.220</i> |
| | GELU | 0.195 | 0.382 | 0.149 | <u>1.520</u> | 0.413 | 0.337 | 0.332 | 0.221 |
| | ReLU | 0.196 | <u>0.380</u> | 0.150 | 1.551 | 0.413 | 0.336 | 0.331 | 0.218 |
| | Sigmoid | <u>0.192</u> | 0.386 | <u>0.146</u> | 1.613 | <u>0.411</u> | 0.325 | <u>0.328</u> | <u>0.216</u> |
| | SiLU | 0.196 | 0.381 | 0.149 | 1.559 | 0.413 | 0.337 | 0.333 | 0.221 |
| | Tanh | 0.187 | 0.375 | 0.141 | 1.447 | 0.410 | <u>0.329</u> | 0.325 | 0.212 |
| Transformer | <i>Linear</i> | <i>0.835</i> | <i>0.748</i> | <i>0.296</i> | <i>4.832</i> | <i>1.328</i> | <i>1.152</i> | <i>1.138</i> | <i>1.389</i> |
| | GELU | <u>0.804</u> | 0.726 | 0.302 | 4.129 | <u>1.269</u> | 1.134 | 1.134 | 1.353 |
| | ReLU | 0.839 | 0.735 | <u>0.272</u> | 4.224 | 1.314 | <u>1.102</u> | 1.116 | 1.382 |
| | Sigmoid | 0.811 | 0.714 | 0.278 | 4.972 | 1.285 | 1.086 | 1.132 | <u>1.357</u> |
| | SiLU | 0.823 | 0.756 | 0.293 | 4.535 | 1.334 | 1.157 | 1.153 | 1.379 |
| | Tanh | 0.797 | <u>0.721</u> | 0.269 | 4.216 | 1.255 | 1.114 | 1.125 | 1.364 |

employing nonlinear activation functions in the proposed active-attention mechanism (20). Our experiments span large-scale image classification tasks on CIFAR-10 [18] and ImageNet [34], language modeling on WikiText-103 [23], and multivariate time series forecasting across 8 different benchmarks. We evaluate the impact of five commonly used activation functions, including ReLU [1], GELU [13], SiLU [9], Sigmoid, and Tanh [28]. Figures 2 (a) and (b) present the results of image classification using different activation functions in self-attention, with ViT [7] and CaiT [37] as the base models. For CIFAR-10, we employed the ViT-Tiny and CaiT-Tiny models, while for ImageNet, we utilized the ViT-Base and CaiT-Medium models. Figure 2 (c) displays the results of the large-scale language modeling task on WikiText-103, using the standard multi-head self-attention transformer [39]. Additionally, we tested various activation functions on the Performer model [5] as another backbone. Our findings show that the GELU and ReLU activation functions greatly improve performance compared to linear activation functions. This aligns with prior research, suggesting that these two activation functions are preferred in large-scale deep networks due to their ability to support more efficient and stable training.

Table 2 further evaluates the impact of different activation functions on transformer-based time-series forecasting models across eight forecasting tasks. In this experiment, we employ the state-of-the-art PatchTST model [27] and the standard self-attention transformer as the backbone. Unlike the results observed in Figure 2, in addition to GELU, we find that Tanh and Sigmoid functions also show prominent advantages over linear activation function. We hypothesize that this is due to the smoothing gradients provided by Tanh and Sigmoid, which may help in capturing subtle patterns in time-series data. Additionally, since these tasks tend to be smaller and more prone to overfitting, the saturation effects of Tanh and Sigmoid could serve as a regularization mechanism by limiting output ranges and avoiding extreme activations.

Quadratic gating versus linear gating. We performed experiments using GPT2 (124M) [31] MoE models on a dataset consisting of 10 billion tokens from FineWeb-Edu [29]. We focus on a GPT2 MoE model featuring 8 experts and a Top2 router with a quadratic gating network. In addition, we considered a linear gating MoE model and a dense GPT2 model for baseline comparisons. The hidden size of the experts is chosen so that all models have approximately the same number of activated parameters. Please refer to Appendix F for more details.

The tested models, along with the baselines, were evaluated on the HellaSwag benchmark. The GPT2-MoE model with a Top2 quadratic router achieved better performance than the dense model and the MoE model with linear gating, based on validation loss and HellaSwag accuracy.

Table 3: Comparison of GPT2-MoE performance (using linear and quadratic gating) against baseline models on the HellaSwag benchmark.

| Model | Val. Loss | HellaSwag (%) |
|-----------------|---------------|---------------|
| Dense | 3.0211 | 30.74% |
| MoE (linear) | 2.9928 | 29.95% |
| MoE (quadratic) | 2.9712 | 32.11% |

6 Discussion

In this paper, we first establish a link between the MoE framework and attention mechanisms. We introduce a formal attention-based approach for the MoE framework and show that quadratic gating in the MoE framework can be interpreted as a self-attention mechanism. Next, we carry out the convergence analysis of parameter and expert estimation under the MoE models with the quadratic polynomial gate and the quadratic monomial gate. Our theories indicate that experts formulated as neural networks with popular activation functions such as ReLU and tanh have faster estimation rates than linear experts. The insights from the theories lead to the new attention mechanism, named active-attention, where we replace the linear value matrix in the attention by non-linear value matrix. Through extensive empirical evaluation, we show the favorable performance of the proposed active-attention over standard attention in various tasks.

Supplement to “Quadratic Gating Functions in Mixture of Experts: A Statistical Insight”

In this supplementary material, we first discuss related works to the quadratic gating MoE model in Section A. Then, in Section C, we provide a convergence analysis for parameter and expert estimation under the quadratic gating mixture of linear experts. Full proofs for the theoretical results of Section 3 and Appendix C are presented in Appendix D. Next, we study the identifiability of the quadratic gating MoE in Appendix E. Lastly, we specify the experimental details for Figure 1 in Appendix F.

A Related Works

A more generalized version of quadratic MoE was first introduced as an alternative model for MoE, utilizing a distinct parametric structure in the gating network [40]. The proposed modified gating network is given by

$$g_i(\mathbf{x}; \Theta_g) = \frac{\pi_i p(\mathbf{x} | \boldsymbol{\theta}_i)}{\sum_{j=1}^N \pi_j p(\mathbf{x} | \boldsymbol{\theta}_j)}, \quad i = 1, \dots, N, \quad (21)$$

where $(\pi_1, \dots, \pi_N)^\top \in \Delta^{N-1}$, and $\Theta_g = \{(\pi_i, \boldsymbol{\theta}_i), i = 1, \dots, N\}$ represents the learnable parameters, with each $p(\mathbf{x} | \boldsymbol{\theta}_i)$ being a density function from the exponential family. The gating function in equation (21) is a nonlinear variant of the softmax linear gating function. In particular, if we assume that $p(\mathbf{x} | \boldsymbol{\theta}_i)$ is a Gaussian density function with mean $\boldsymbol{\mu}_i \in \mathbb{R}^d$ and covariance matrix $\boldsymbol{\Sigma}_i \in \mathbb{R}^{d \times d}$, this leads to a specific form of quadratic softmax gating function. Here, it is assumed that the covariance matrices are positive definite. Observe that setting $\boldsymbol{\Sigma}_i = \boldsymbol{\Sigma}$ for all $i \in [N]$ reinstates the linear gating model.

The gating function $g_i(\mathbf{x}; \Theta_g)$ essentially models the posterior probability $\mathbb{P}(\zeta = i | \mathbf{x})$, indicating the likelihood that \mathbf{x} is assigned to the partition associated with the i -th expert. Here, $\zeta \in \{1, \dots, N\}$ is a latent gating variable that selects a particular expert. More precisely, the gating function defined in Equation (21) interprets this posterior probability when ζ follows a categorical distribution with parameters $(\pi_1, \dots, \pi_N)^\top \in \Delta^{N-1}$, and conditioned on the event that ζ selects the i th expert, the distribution of \mathbf{x} is modeled by a specific parametric distribution $p(\cdot | \boldsymbol{\theta}_i)$. Motivated by this interpretation of gating function, [21] proposed the *Quadratically Gated Mixture of Experts*, in which the parametric distribution $p(\cdot | \boldsymbol{\theta}_i)$ is assumed to follow a Gaussian density.

B Quadratic Monomial Gate

In this section, we proceed to streamline the analysis of the quadratic monomial gating based on the regression framework in equation (10). Due to the change of the gating function, the corresponding regression function is reformulated as follows:

$$\tilde{f}_{G_*}(\mathbf{x}) := \sum_{i=1}^{N^*} \frac{\exp(\mathbf{x}^\top \mathbf{A}_i^* \mathbf{x} + c_i^*)}{\sum_{j=1}^{N^*} \exp(\mathbf{x}^\top \mathbf{A}_j^* \mathbf{x} + c_j^*)} \cdot h(\mathbf{x}, \boldsymbol{\eta}_i^*). \quad (22)$$

In comparison with the quadratic polynomial gating, the first-degree monomial term $b^\top \mathbf{x}$ has been removed from the scoring function. As a consequence, the least squares estimator under this setting

also changes accordingly to

$$\tilde{G}_n := \arg \min_{G \in \mathcal{G}_N(\Theta)} \sum_{i=1}^n \left(y_i - \tilde{f}_G(\mathbf{x}_i) \right)^2. \quad (23)$$

Given the above estimator, we provide in Theorem B.1 the convergence rate of regression estimation $\tilde{f}_{\tilde{G}_n}(\cdot)$ to the regression function $\tilde{f}_{G_*}(\cdot)$.

Theorem B.1 (Regression Estimation Rate). *Equipped with a least squares estimator \tilde{G}_n given in equation (23), the model estimation $\tilde{f}_{\tilde{G}_n}$ converges to the true model \tilde{f}_{G_*} at the following rate:*

$$\|\tilde{f}_{\tilde{G}_n} - \tilde{f}_{G_*}\|_{L_2(\mu)} = \tilde{\mathcal{O}}_P(n^{-1/2}). \quad (24)$$

See Appendix D.4 for the proof of Theorem B.1. It follows from the bound (24) that the regression estimation rate still remains parametric on the sample size, which matches that in Theorem 3.1 where we use the quadratic polynomial gating function in the MoE-type regression function.

Analogous to Section 3.1, we also derive a *mono-strong identifiability condition* in Definition B.2 to determine which expert functions will have faster estimation rates than others.

Definition B.2 (Mono-strong identifiability). We say that an expert function $x \mapsto h(\mathbf{x}, \boldsymbol{\eta})$ is strongly identifiable if it is twice differentiable w.r.t its parameter $\boldsymbol{\eta}$, and if for any $k \geq 1$ and pair-wise different $\boldsymbol{\eta}_1, \dots, \boldsymbol{\eta}_k$, the following set

$$\left\{ x^\nu \cdot \frac{\partial^{|\gamma|} h}{\partial \boldsymbol{\eta}^\gamma}(\mathbf{x}; \boldsymbol{\eta}_j) : j \in [k], \nu \in \mathbb{N}^d, \gamma \in \mathbb{N}^q, |\nu| \in \{0, 2, 4\}, 0 \leq |\gamma| \leq 2 - \frac{|\nu|}{2} \right\},$$

is linearly independent for almost every \mathbf{x} .

Example. It can be verified that the mono-strong identifiability condition holds for experts formulated as feed-forward neural networks with activation functions such as $\text{ReLU}(\cdot)$ and $\tanh(\cdot)$. However, a linear expert fails to satisfy this condition.

Voronoi loss. Now, we aim to establish the convergence rate of parameter and expert estimation under the mixture of strongly identifiable experts model with the quadratic monomial gating function. For that sake, let us design a new Voronoi loss function among parameters defined as below.

$$\begin{aligned} \mathcal{L}_3(G, G_*) := & \sum_{j:|\mathcal{V}_j|>1} \sum_{i \in \mathcal{V}_j} \exp(c_i) \left[\|\Delta \mathbf{A}_{ij}\|^2 + \|\Delta \boldsymbol{\eta}_{ij}\|^2 \right] \\ & + \sum_{j:|\mathcal{V}_j|=1} \sum_{i \in \mathcal{V}_j} \exp(c_i) \left[\|\Delta \mathbf{A}_{ij}\| + \|\Delta \boldsymbol{\eta}_{ij}\| \right] \\ & + \sum_{j=1}^{N^*} \left| \sum_{i \in \mathcal{V}_j} \exp(c_i) - \exp(c_j^*) \right|. \end{aligned} \quad (25)$$

Now, we are ready to capture the parameter and expert estimation rates in Theorem B.3.

Theorem B.3. Assume that the expert function $h(\mathbf{x}, \boldsymbol{\eta})$ is strongly identifiable, then we achieve the following lower bound for any $G \in \mathcal{G}_k(\Theta)$:

$$\|\tilde{f}_G - \tilde{f}_{G_*}\|_{L_2(\mu)} \gtrsim \mathcal{L}_3(G, G_*),$$

which together with Theorem 3.1 indicates that $\mathcal{L}_3(\tilde{G}_n, G_*) = \tilde{\mathcal{O}}_P(n^{-1/2})$.

Proof of Theorem B.3 is in Appendix D.5. A few comments regarding this theorem are in order: (i) The rates for estimating gating parameters \mathbf{A}_j^* fitted by more than one atom, i.e. $|\mathcal{V}_j(\tilde{G}_n)| > 1$, are significantly improved to be of order $\tilde{\mathcal{O}}_P(n^{-1/4})$. Those rates are much faster than their counterparts when using the quadratic polynomial gate, which stand at order $\tilde{\mathcal{O}}_P(n^{-1/\bar{r}(|\mathcal{V}_j|)})$ (cf. Theorem 3.3). This rate acceleration is due to the disappearance of the interaction among gating parameters in equation (14) when using the quadratic monomial gate. Meanwhile, the estimation rates for expert parameters $\boldsymbol{\eta}_j^*$ remained unchanged at order $\tilde{\mathcal{O}}_P(n^{-1/4})$; (ii) Model parameters $\mathbf{A}_j^*, \boldsymbol{\eta}_j^*$ fitted by exactly one atom, i.e. $|\mathcal{V}_j(\tilde{G}_n)| = 1$, enjoy the parametric estimation rates of order $\tilde{\mathcal{O}}_P(n^{-1/2})$, which are comparable to their counterparts in Theorem 3.3.

Mono-weak identifiability of linear experts. Similar to the polynomial quadratic gating, the linear expert $h(\mathbf{x}, (\boldsymbol{\beta}_1, \beta_0)) = (\boldsymbol{\beta}_{1i})^\top \mathbf{x} + \beta_{0i}$ in the monomial quadratic gating setting also does not satisfy the mono-strong identifiability condition. That violation leads to $\mathcal{O}(1/\log(n))$ rates of the parameters and experts under the quadratic monomial gating MoE. The proof for this result is similar to that of Theorem C.1 in Appendix C; therefore, it is omitted.

C Convergence Analysis for the Quadratic Gating Mixture of Linear Experts

In this appendix, we provide the convergence rates for parameter and expert estimation under the MoE model with the quadratic polynomial gate. Meanwhile, the analysis for the quadratic monomial gate can be done in a similar fashion.

As being mentioned in the main text, for the linear expert function $h(\mathbf{x}, (\boldsymbol{\beta}_1, \beta_0)) = (\boldsymbol{\beta}_{1i})^\top \mathbf{x} + \beta_{0i}$, where $(\boldsymbol{\beta}_1, \beta_0) \in \mathbb{R}^d \times \mathbb{R}$, we observe that it violates the strong identifiability condition due to an interaction among parameters via the following partial differential equation:

$$\frac{\partial^2 F}{\partial b \partial \beta_0}(\mathbf{x}; \mathbf{A}, \mathbf{b}, \boldsymbol{\beta}_1, \beta_0) = \frac{\partial F}{\partial \boldsymbol{\beta}_1}(\mathbf{x}; \mathbf{A}_i, \mathbf{b}_i, \boldsymbol{\beta}_1, \beta_0), \quad (26)$$

where we denote $F(\mathbf{x}; \mathbf{A}, \mathbf{b}, \boldsymbol{\beta}_1, \beta_0) := \exp(\mathbf{x}^\top \mathbf{A} \mathbf{x} + \mathbf{b}^\top \mathbf{x})(\boldsymbol{\beta}_1^\top \mathbf{x} + \beta_0)$.

To capture the effects of such parameter interaction on the convergence of parameter estimation, let us design another Voronoi loss tailored to this setting. More specifically, we define for any $r \geq 1$ that

$$\begin{aligned} \mathcal{L}_{2,r}(G, G_*) &:= \sum_{j=1}^{N^*} \sum_{i \in \mathcal{V}_j} \exp(c_i) \left[\|\Delta \mathbf{A}_{ij}\|^r + \|\Delta \mathbf{b}_{ij}\|^r + \|\Delta \boldsymbol{\beta}_{1ij}\|^r + |\Delta \beta_{0ij}|^r \right] \\ &\quad + \sum_{j=1}^{N^*} \left| \sum_{i \in \mathcal{V}_j} \exp(c_i) - \exp(c_j^*) \right|. \end{aligned} \quad (27)$$

Given the above loss function, we demonstrate in the following theorem that the parameter and expert estimation rates are seriously affected by the parameter interaction in equation (26).

Theorem C.1. *Assume that the experts take the form $\beta_1^\top \mathbf{x} + \beta_0$, then we achieve the following minimax lower bound of estimating G_* :*

$$\inf_{\bar{G}_n \in \mathcal{G}_N(\Theta)} \sup_{G \in \mathcal{G}_N(\Theta) \setminus \mathcal{G}_{N^*-1}(\Theta)} \mathbb{E}_{f_G} [\mathcal{L}_{2,r}(\bar{G}_n, G)] \gtrsim n^{-1/2},$$

for any $r \geq 1$, where \mathbb{E}_{f_G} indicates the expectation taken w.r.t the product measure with f_G^n .

Proof of Theorem C.1 is in Appendix D.3. A few remarks on the result of this theorem are in order. First, Theorem C.1 reveals that using linear experts make the estimation rates for all the parameters \mathbf{A}_i^* , \mathbf{b}_i^* , β_{1i}^* and β_{0i}^* are slower than $\tilde{\mathcal{O}}_P(n^{-1/2r})$ for any $r \geq 1$, and could be as slow as $\mathcal{O}_P(1/\log(n))$ owing to the interaction in equation (19). Second, we have that

$$\sup_x \left| ((\hat{\beta}_{1i}^n)^\top \mathbf{x} + \hat{\beta}_{0i}^n) - ((\beta_{1j}^*)^\top \mathbf{x} + \beta_{0j}^*) \right| \leq \sup_{\mathbf{x}} \|\hat{\beta}_{1i}^n - \beta_{1j}^*\| \cdot \|\mathbf{x}\| + |\hat{\beta}_{0i}^n - \beta_{0j}^*|.$$

Since the input space \mathcal{X} is bounded, the rates for estimating linear experts $(\beta_{1j}^*)^\top \mathbf{x} + \beta_{0j}^*$ could also be of order $\mathcal{O}_P(1/\log(n))$. Hence, combining with the result in Theorem 3.3, we deduce that the performance of a mixture of linear experts cannot compare to that of a mixture of non-linear experts in terms of the expert estimation problem. This observation totally aligns with the findings in [4].

D Proof of Theoretical Results

In this appendix, we present the detailed proofs for the theoretical results introduced in the paper.

D.1 Proof of Theorem 3.1

For the proof of the theorem, we first introduce some notation. Firstly, we denote by $\mathcal{F}_k(\Theta)$ the set of conditional densities of all mixing measures in $\mathcal{G}_k(\Theta)$, that is, $\mathcal{F}_k(\Theta) := \{f_G(\mathbf{x}) : G \in \mathcal{G}_N(\Theta)\}$. Additionally, for each $\delta > 0$, the $L_2(\mu)$ ball centered around the regression function $f_{G_*}(\mathbf{x})$ and intersected with the set $\mathcal{F}_k(\Theta)$ is defined as

$$\mathcal{F}_k(\Theta, \delta) := \{f \in \mathcal{F}_k(\Theta) : \|f - f_{G_*}\|_{L_2(\mu)} \leq \delta\}.$$

In order to measure the size of the above set, Geer et. al. [38] suggest using the following quantity:

$$\mathcal{J}_B(\delta, \mathcal{F}_k(\Theta, \delta)) := \int_{\delta^2/2^{13}}^{\delta} H_B^{1/2}(t, \mathcal{F}_k(\Theta, t), \|\cdot\|_{L_2(\mu)}) dt \vee \delta, \quad (28)$$

where $H_B(t, \mathcal{F}_k(\Theta, t), \|\cdot\|_{L_2(\mu)})$ stands for the bracketing entropy [38] of $\mathcal{F}_k(\Theta, t)$ under the L^2 -norm, and $t \vee \delta := \max\{t, \delta\}$. By using the similar proof argument of Theorem 7.4 and Theorem 9.2 in [38] with notations being adapted to this work, we obtain the following lemma:

Lemma D.1. *Take $\Psi(\delta) \geq \mathcal{J}_B(\delta, \mathcal{F}_k(\Theta, \delta))$ that satisfies $\Psi(\delta)/\delta^2$ is a non-increasing function of δ . Then, for some universal constant c and for some sequence (δ_n) such that $\sqrt{n}\delta_n^2 \geq c\Psi(\delta_n)$, we achieve that*

$$\mathbb{P}\left(\|f_{\hat{G}_n} - f_{G_*}\|_{L_2(\mu)} > \delta\right) \leq c \exp\left(-\frac{n\delta^2}{c^2}\right),$$

for all $\delta \geq \delta_n$.

We now demonstrate that when the expert functions are Lipschitz continuous, the following bound holds:

$$H_B(\varepsilon, \mathcal{F}_k(\Theta), \|\cdot\|_{L^2(\mu)}) \lesssim \log(1/\varepsilon), \quad (29)$$

for any $0 < \varepsilon \leq 1/2$. Indeed, for any function $f_G \in \mathcal{F}_k(\Theta)$, since the expert functions are bounded, we obtain that $f_G(\mathbf{x}) \leq M$ for almost everywhere \mathbf{x} , where M is bounded constant of the expert functions. Let $\tau \leq \varepsilon$ and $\{\pi_1, \dots, \pi_N\}$ be the τ -cover under the L^2 norm of the set $\mathcal{F}_k(\Theta)$ where $N := N(\tau, \mathcal{F}_k(\Theta), \|\cdot\|_{L^2(\mu)})$ is the η -covering number of the metric space $(\mathcal{F}_k(\Theta), \|\cdot\|_{L^2(\mu)})$. Then, we construct the brackets of the form $[L_i(\mathbf{x}), U_i(\mathbf{x})]$ for all $i \in [N]$ as follows:

$$\begin{aligned} L_i(\mathbf{x}) &:= \max\{\pi_i(\mathbf{x}) - \tau, 0\}, \\ U_i(\mathbf{x}) &:= \max\{\pi_i(\mathbf{x}) + \tau, M\}. \end{aligned}$$

From the above construction, we can validate that $\mathcal{F}_k(\Theta) \subset \bigcup_{i=1}^N [L_i(\mathbf{x}), U_i(\mathbf{x})]$ and $U_i(\mathbf{x}) - L_i(\mathbf{x}) \leq 2\min\{2\tau, M\}$. Therefore, it follows that

$$\|U_i - L_i\|_{L^2(\mu)}^2 = \int (U_i - L_i)^2 d\mu(\mathbf{x}) \leq \int 16\tau^2 d\mu(\mathbf{x}) = 16\tau^2,$$

which implies that $\|U_i - L_i\|_{L^2(\mu)} \leq 4\tau$. By definition of the bracketing entropy, we deduce that

$$H_B(4\tau, \mathcal{F}_k(\Theta), \|\cdot\|_{L^2(\mu)}) \leq \log N = \log N(\tau, \mathcal{F}_k(\Theta), \|\cdot\|_{L^2(\mu)}). \quad (30)$$

Therefore, we need to provide an upper bound for the covering number N . In particular, we denote $\Delta := \{(A, b, c) \in \mathbb{R}^{d \times d} \times \mathbb{R}^d \times \mathbb{R} : (A, b, c, \eta) \in \Theta\}$ and $\Omega := \{\eta \in \mathbb{R}^q : (A, b, c, \eta) \in \Theta\}$. Since Θ is a compact set, Δ and Ω are also compact. Therefore, we can find τ -covers Δ_τ and Ω_τ for Δ and Ω , respectively. We can check that

$$|\Delta_\tau| \leq \mathcal{O}_P(\tau^{-(d^2+d+1)k}), \quad |\Omega_\tau| \lesssim \mathcal{O}_P(\tau^{-qk}).$$

For each mixing measure $G = \sum_{i=1}^k \exp(c_i) \delta_{(\mathbf{A}_i, \mathbf{b}_i, \eta_i)} \in \mathcal{G}_k(\Theta)$, we consider other two mixing measures:

$$\check{G} := \sum_{i=1}^k \exp(c_i) \delta_{(\mathbf{A}_i, \mathbf{b}_i, \bar{\eta}_i)}, \quad \bar{G} := \sum_{i=1}^k \exp(\bar{c}_i) \delta_{(\bar{A}_i, \bar{b}_i, \bar{\eta}_i)}.$$

Here, $\bar{\eta}_i \in \Omega_\tau$ such that $\bar{\eta}_i$ is the closest to η_i in that set, while $(\bar{A}_i, \bar{b}_i, \bar{c}_i) \in \Delta_\tau$ is the closest to $(\mathbf{A}_i, \mathbf{b}_i, c_i)$ in that set. From the above formulations, we get that

$$\begin{aligned} \|f_G - f_{\check{G}}\|_{L^2(\mu)}^2 &= \int \left[\sum_{i=1}^k \frac{\exp(\mathbf{x}^\top \mathbf{A}_i \mathbf{x} + (\mathbf{b}_i)^\top \mathbf{x} + c_i)}{\sum_{j=1}^k \exp(\mathbf{x}^\top \mathbf{A}_j \mathbf{x} + (\mathbf{b}_j)^\top \mathbf{x} + c_j)} \cdot [h(\mathbf{x}, \eta_i) - h(\mathbf{x}, \bar{\eta}_i)] \right]^2 d\mu(\mathbf{x}) \\ &\leq k \int \sum_{i=1}^k \left[\frac{\exp(\mathbf{x}^\top \mathbf{A}_i \mathbf{x} + (\mathbf{b}_i)^\top \mathbf{x} + c_i)}{\sum_{j=1}^k \exp(\mathbf{x}^\top \mathbf{A}_j \mathbf{x} + (\mathbf{b}_j)^\top \mathbf{x} + c_j)} \cdot [h(\mathbf{x}, \eta_i) - h(\mathbf{x}, \bar{\eta}_i)] \right]^2 d\mu(\mathbf{x}) \\ &\leq k \int \sum_{i=1}^k [h(\mathbf{x}, \eta_i) - h(\mathbf{x}, \bar{\eta}_i)]^2 d\mu(\mathbf{x}) \\ &\leq k \int \sum_{i=1}^k [L_1 \cdot \|\eta_i - \bar{\eta}_i\|]^2 d\mu(\mathbf{x}) \\ &\leq (kL_1\tau)^2, \end{aligned}$$

which indicates that $\|f_G - f_{\check{G}}\|_{L_2(\mu)} \leq L_1 k \tau$. Here, the second inequality is according to the Cauchy-Schwarz inequality, the third inequality occurs as the softmax weight is bounded by 1, and the fourth inequality follows from the fact that the expert $h(\mathbf{x}, \cdot)$ is a Lipschitz function with Lipschitz constant L_1 . Next, we have

$$\begin{aligned}
\|f_{\check{G}} - f_{\bar{G}}\|_{L_2(\mu)}^2 &\leq k \int \sum_{i=1}^k \left[\left(\frac{\exp(\mathbf{x}^\top \mathbf{A}_i \mathbf{x} + (\mathbf{b}_i)^\top \mathbf{x} + c_i)}{\sum_{j=1}^k \exp(\mathbf{x}^\top \mathbf{A}_j \mathbf{x} + (\mathbf{b}_j)^\top \mathbf{x} + c_j)} \right. \right. \\
&\quad \left. \left. - \frac{\exp(\mathbf{x}^\top \bar{\mathbf{A}}_i \mathbf{x} + (\bar{\mathbf{b}}_i)^\top \mathbf{x} + \bar{c}_i)}{\sum_{j=1}^k \exp(\mathbf{x}^\top \bar{\mathbf{A}}_j \mathbf{x} + (\bar{\mathbf{b}}_j)^\top \mathbf{x} + \bar{c}_j)} \right) \cdot h(\mathbf{x}, \bar{\boldsymbol{\eta}}_i) \right]^2 d\mu(\mathbf{x}) \\
&\leq k M^2 L^2 \int \sum_{i=1}^k \left[\|A_i - \bar{A}_i\| \cdot \|x\|^2 + \|\mathbf{b}_i - \bar{\mathbf{b}}_i\| \cdot \|x\| + |c_i - \bar{c}_i| \right]^2 d\mu(\mathbf{x}) \\
&\leq k M^2 L^2 \int \sum_{i=1}^k (\tau B^2 + \tau B + \tau)^2 d\mu(\mathbf{x}) \\
&\leq [k M L \tau (B^2 + B + 1)]^2,
\end{aligned}$$

where $L \geq 0$ is a Lipschitz constant of the softmax weight. This result implies that $\|f_{\check{G}} - f_{\bar{G}}\|_{L_2(\mu)} \leq k M L (B^2 + B + 1) \tau$. According to the triangle inequality, we have

$$\|f_G - f_{\bar{G}}\|_{L_2(\mu)} \leq \|f_G - f_{\check{G}}\|_{L_2(\mu)} + \|f_{\check{G}} - f_{\bar{G}}\|_{L_2(\mu)} \leq [L_1 k + k M L (B^2 + B + 1)] \cdot \tau.$$

By definition of the covering number, we deduce that

$$N(\tau, \mathcal{F}_k(\Theta), \|\cdot\|_{L_2(\mu)}) \leq |\Delta_\tau| \times |\Omega_\tau| \leq \mathcal{O}_P(n^{-(d^2+d+1)k}) \times \mathcal{O}(n^{-qk}) \leq \mathcal{O}(n^{-(d^2+d+1+q)k}). \quad (31)$$

Combine equations (30) and (31), we achieve that

$$H_B(4\tau, \mathcal{F}_k(\Theta), \|\cdot\|_{L_2(\mu)}) \lesssim \log(1/\tau).$$

Let $\tau = \varepsilon/4$, then we obtain that

$$H_B(\varepsilon, \mathcal{F}_k(\Theta), \|\cdot\|_{L_2(\mu)}) \lesssim \log(1/\varepsilon).$$

As a result, it follows that

$$\mathcal{J}_B(\delta, \mathcal{F}_k(\Theta, \delta)) = \int_{\delta^2/2^{13}}^{\delta} H_B^{1/2}(t, \mathcal{F}_k(\Theta, t), \|\cdot\|_{L_2(\mu)}) dt \vee \delta \lesssim \int_{\delta^2/2^{13}}^{\delta} \log(1/t) dt \vee \delta. \quad (32)$$

Let $\Psi(\delta) = \delta \cdot [\log(1/\delta)]^{1/2}$, then $\Psi(\delta)/\delta^2$ is a non-increasing function of δ . Furthermore, equation (32) indicates that $\Psi(\delta) \geq \mathcal{J}_B(\delta, \mathcal{F}_k(\Theta, \delta))$. In addition, let $\delta_n = \sqrt{\log(n)/n}$, then we get that $\sqrt{n}\delta_n^2 \geq c\Psi(\delta_n)$ for some universal constant c . Finally, by applying Lemma D.1, we achieve the desired conclusion of the theorem.

D.2 Proof of Theorem 3.3

In this proof, we aim to establish the following inequality:

$$\inf_{G \in \mathcal{G}_N(\Theta)} \|f_G - f_{G_*}\|_{L_2(\mu)} / \mathcal{L}_1(G, G_*) > 0. \quad (33)$$

For that purpose, we divide the proof of the above inequality into local and global parts in the sequel.

Local part: In this part, we demonstrate that

$$\lim_{\varepsilon \rightarrow 0} \inf_{G \in \mathcal{G}_N(\Theta): \mathcal{L}_1(G, G_*) \leq \varepsilon} \|f_G - f_{G_*}\|_{L_2(\mu)} / \mathcal{L}_1(G, G_*) > 0. \quad (34)$$

Assume by contrary that the above inequality does not hold true, then there exists a sequence of mixing measures $G_n = \sum_{i=1}^{N^*} \exp(c_i^n) \delta_{(\mathbf{A}_i^n, \mathbf{b}_i^n, \boldsymbol{\eta}_i^n)}$ in $\mathcal{G}_N(\Theta)$ such that $\mathcal{L}_{1n} := \mathcal{L}_1(G_n, G_*) \rightarrow 0$ and

$$\|f_{G_n} - f_{G_*}\|_{L_2(\mu)} / \mathcal{L}_{1n} \rightarrow 0, \quad (35)$$

as $n \rightarrow \infty$. Let us denote by $\mathcal{V}_j^n := \mathcal{V}_j(G_n)$ a Voronoi cell of G_n generated by the j -th components of G_* . Since our arguments are asymptotic, we may assume that those Voronoi cells do not depend on the sample size, i.e. $\mathcal{V}_j = \mathcal{V}_j^n$. Thus, the Voronoi loss \mathcal{L}_{1n} can be represented as

$$\begin{aligned} \mathcal{L}_{1n} := & \sum_{j: |\mathcal{V}_j| > 1} \sum_{i \in \mathcal{V}_j} \exp(c_i^n) \left[\|\Delta \mathbf{A}_{ij}^n\|^{-\frac{\bar{r}(|\mathcal{V}_j|)}{2}} + \|\Delta \mathbf{b}_{ij}^n\|^{\bar{r}(|\mathcal{V}_j|)} + \|\Delta \boldsymbol{\eta}_{ij}^n\|^2 \right] \\ & + \sum_{j: |\mathcal{V}_j| = 1} \sum_{i \in \mathcal{V}_j} \exp(c_i^n) \left[\|\Delta \mathbf{A}_{ij}^n\| + \|\Delta \mathbf{b}_{ij}^n\| + \|\Delta \boldsymbol{\eta}_{ij}^n\| \right] + \sum_{j=1}^{N^*} \left| \sum_{i \in \mathcal{V}_j} \exp(c_i^n) - \exp(c_j^*) \right|, \end{aligned} \quad (36)$$

where we denote $\Delta \mathbf{A}_{ij}^n := \mathbf{A}_i^n - \mathbf{A}_j^*$, $\Delta \mathbf{b}_{ij}^n := \mathbf{b}_i^n - \mathbf{b}_j^*$ and $\Delta \boldsymbol{\eta}_{ij}^n := \boldsymbol{\eta}_i^n - \boldsymbol{\eta}_j^*$.

Since $\mathcal{L}_{1n} \rightarrow 0$, we get that $(\mathbf{A}_i^n, \mathbf{b}_i^n, \boldsymbol{\eta}_i^n) \rightarrow (\mathbf{A}_j^*, \mathbf{b}_j^*, \boldsymbol{\eta}_j^*)$ and $\sum_{i \in \mathcal{V}_j} \exp(c_i^n) \rightarrow \exp(c_j^*)$ as $n \rightarrow \infty$ for any $i \in \mathcal{V}_j$ and $j \in [N^*]$. Now, we divide the proof of local part into three steps as follows:

Step 1 - Taylor expansion. In this step, we decompose the term

$$Q_n(\mathbf{x}) := \left[\sum_{j=1}^{N^*} \exp(\mathbf{x}^\top \mathbf{A}_j^* \mathbf{x} + (\mathbf{b}_j^*)^\top \mathbf{x} + c_j^*) \right] \cdot [f_{G_n}(\mathbf{x}) - f_{G_*}(\mathbf{x})] \quad (37)$$

into a combination of linearly independent elements using Taylor expansion. In particular, we have

$$\begin{aligned} Q_n(\mathbf{x}) = & \sum_{j=1}^{N^*} \sum_{i \in \mathcal{V}_j} \exp(c_i^n) \left[\exp(\mathbf{x}^\top \mathbf{A}_i^n \mathbf{x} + (\mathbf{b}_i^n)^\top \mathbf{x}) h(\mathbf{x}; \boldsymbol{\eta}_i^n) - \exp(\mathbf{x}^\top \mathbf{A}_j^* \mathbf{x} + (\mathbf{b}_j^*)^\top \mathbf{x}) h(\mathbf{x}; \boldsymbol{\eta}_j^*) \right] \\ & - \sum_{j=1}^{N^*} \sum_{i \in \mathcal{V}_j} \exp(c_i^n) \left[\exp(\mathbf{x}^\top \mathbf{A}_i^n \mathbf{x} + (\mathbf{b}_i^n)^\top \mathbf{x}) - \exp(\mathbf{x}^\top \mathbf{A}_j^* \mathbf{x} + (\mathbf{b}_j^*)^\top \mathbf{x}) \right] f_{G_n}(\mathbf{x}) \\ & + \sum_{j=1}^{N^*} \left(\sum_{i \in \mathcal{V}_j} \exp(c_i^n) - \exp(c_j^*) \right) \left[\exp(\mathbf{x}^\top \mathbf{A}_j^* \mathbf{x} + (\mathbf{b}_j^*)^\top \mathbf{x}) h(\mathbf{x}; \boldsymbol{\eta}_j^*) - \exp(\mathbf{x}^\top \mathbf{A}_j^* \mathbf{x} + (\mathbf{b}_j^*)^\top \mathbf{x}) f_{G_n}(\mathbf{x}) \right] \\ & := A_n(\mathbf{x}) - B_n(\mathbf{x}) + C_n(\mathbf{x}). \end{aligned} \quad (38)$$

Decomposition of A_n . Next, we continue to separate the term A_n into two parts as follows:

$$\begin{aligned} A_n(\mathbf{x}) &:= \sum_{j:|\mathcal{V}_j|=1} \sum_{i \in \mathcal{V}_j} \exp(c_i^n) \left[\exp(\mathbf{x}^\top A_i^n \mathbf{x} + (b_i^n)^\top \mathbf{x}) h(\mathbf{x}; \eta_i^n) - \exp(\mathbf{x}^\top \mathbf{A}_j^* \mathbf{x} + (\mathbf{b}_j^*)^\top \mathbf{x}) h(\mathbf{x}; \boldsymbol{\eta}_j^*) \right] \\ &+ \sum_{j:|\mathcal{V}_j|>1} \sum_{i \in \mathcal{V}_j} \exp(c_i^n) \left[\exp(\mathbf{x}^\top A_i^n \mathbf{x} + (b_i^n)^\top \mathbf{x}) h(\mathbf{x}; \eta_i^n) - \exp(\mathbf{x}^\top \mathbf{A}_j^* \mathbf{x} + (\mathbf{b}_j^*)^\top \mathbf{x}) h(\mathbf{x}; \boldsymbol{\eta}_j^*) \right] \\ &:= A_{n,1}(\mathbf{x}) + A_{n,2}(\mathbf{x}). \end{aligned}$$

Let $E(\mathbf{x}; A, b) := \exp(\mathbf{x}^\top A \mathbf{x} + b^\top \mathbf{x})$. By means of the first-order Taylor expansion, we have

$$\begin{aligned} A_{n,1}(\mathbf{x}) &= \sum_{j:|\mathcal{V}_j|=1} \sum_{i \in \mathcal{V}_j} \frac{\exp(c_i^n)}{\alpha!} \sum_{|\alpha|=1} (\Delta A_{ij}^n)^{\alpha_1} (\Delta \mathbf{b}_{ij}^n)^{\alpha_2} (\Delta \boldsymbol{\eta}_{ij}^n)^{\alpha_3} \\ &\quad \times \frac{\partial^{|\alpha_1|+|\alpha_2|} E}{\partial A^{\alpha_1} \partial b^{\alpha_2}}(\mathbf{x}; \mathbf{A}_j^*, \mathbf{b}_j^*) \frac{\partial^{|\alpha_3|} h}{\partial \boldsymbol{\eta}^{\alpha_3}}(\mathbf{x}; \boldsymbol{\eta}_j^*) + R_{n,1}(\mathbf{x}), \end{aligned}$$

where $R_{n,1}(\mathbf{x})$ is a Taylor remainder such that $R_{n,1}(\mathbf{x})/\mathcal{L}_{1n} \rightarrow 0$ as $n \rightarrow \infty$. Note that

$$\frac{\partial^{|\alpha_1|+|\alpha_2|} E}{\partial A^{\alpha_1} \partial b^{\alpha_2}}(\mathbf{x}; \mathbf{A}_j^*, \mathbf{b}_j^*) = \frac{\partial^{2|\alpha_1|+|\alpha_2|} E}{\partial b^{\tau(\alpha_1, \alpha_2)}}(\mathbf{x}; \mathbf{A}_j^*, \mathbf{b}_j^*),$$

where $\tau(\alpha_1, \alpha_2) := \left(\sum_{u=1}^d (\alpha_1^{(uv)} + \alpha_1^{(vu)}) + \alpha_2^{(v)} \right)_{v=1}^d = \left(2 \sum_{u=1}^d \alpha_1^{(uv)} + \alpha_2^{(v)} \right)_{v=1}^d \in \mathbb{N}^d$. Then, $A_{n,1}(\mathbf{x})$ can be rewritten as

$$\begin{aligned} A_{n,1}(\mathbf{x}) &= \sum_{j:|\mathcal{V}_j|=1} \sum_{|\alpha_3|=0}^1 \sum_{|\ell_1|=0 \vee 1-|\alpha_3|}^{2(1-|\alpha_3|)} \sum_{i \in \mathcal{V}_j} \sum_{\tau(\alpha_1, \alpha_2)=\ell_1} \frac{\exp(c_i^n)}{\alpha!} (\Delta A_{ij}^n)^{\alpha_1} (\Delta \mathbf{b}_{ij}^n)^{\alpha_2} (\Delta \boldsymbol{\eta}_{ij}^n)^{\alpha_3} \\ &\quad \times \frac{\partial^{2|\alpha_1|+|\alpha_2|} E}{\partial b^{\tau(\alpha_1, \alpha_2)}}(\mathbf{x}; \mathbf{A}_j^*, \mathbf{b}_j^*) \frac{\partial^{|\alpha_3|} h}{\partial \boldsymbol{\eta}^{\alpha_3}}(\mathbf{x}; \boldsymbol{\eta}_j^*) + R_{n,1}(\mathbf{x}) \\ &= \sum_{j:|\mathcal{V}_j|=1} \sum_{|\alpha_3|=0}^1 \sum_{|\ell_1|=0 \vee 1-|\alpha_3|}^{2(1-|\alpha_3|)} S_{n,j,\alpha_3,\ell_1} \cdot \frac{\partial^{|\ell_1|} E}{\partial b^{\ell_1}}(\mathbf{x}; \mathbf{A}_j^*, \mathbf{b}_j^*) \frac{\partial^{|\alpha_3|} h}{\partial \boldsymbol{\eta}^{\alpha_3}}(\mathbf{x}; \boldsymbol{\eta}_j^*) + R_{n,1}(\mathbf{x}), \end{aligned}$$

where we denote

$$S_{n,j,\alpha_3,\ell_1} := \sum_{i \in \mathcal{V}_j} \sum_{\tau(\alpha_1, \alpha_2)=\ell_1} \frac{\exp(c_i^n)}{\alpha!} (\Delta A_{ij}^n)^{\alpha_1} (\Delta \mathbf{b}_{ij}^n)^{\alpha_2} (\Delta \boldsymbol{\eta}_{ij}^n)^{\alpha_3}$$

for any $j \in [N^*]$ and $(\alpha_3, \ell_1) \neq (\mathbf{0}_d, \mathbf{0}_d)$.

Analogously, by applying the Taylor expansion of order $\bar{r}_j := \bar{r}(|\mathcal{V}_j|)$, we can represent the term $A_{n,2}(\mathbf{x})$ as

$$A_{n,2}(\mathbf{x}) = \sum_{j:|\mathcal{V}_j|>1} \sum_{|\alpha_3|=0}^{\bar{r}_j} \sum_{|\ell_1|=0 \vee 1-|\alpha_3|}^{2(\bar{r}_j-|\alpha_3|)} S_{n,j,\alpha_3,\ell_1} \cdot \frac{\partial^{|\ell_1|} E}{\partial b^{\ell_1}}(\mathbf{x}; \mathbf{A}_j^*, \mathbf{b}_j^*) \frac{\partial^{|\alpha_3|} h}{\partial \boldsymbol{\eta}^{\alpha_3}}(\mathbf{x}; \boldsymbol{\eta}_j^*) + R_{n,2}(\mathbf{x}),$$

where $R_{n,2}(\mathbf{x})$ is a Taylor remainder such that $R_{n,2}(\mathbf{x})/\mathcal{L}_{1n} \rightarrow 0$ as $n \rightarrow \infty$.

Decomposition of B_n . Note that $B_n(\mathbf{x})$ can be rewritten as

$$\begin{aligned} B_n(\mathbf{x}) &= \sum_{j:|\mathcal{V}_j|=1} \sum_{i \in \mathcal{V}_j} \exp(c_i^n) \left[E(\mathbf{x}; A_i^n, b_i^n) - E(\mathbf{x}; \mathbf{A}_j^*, \mathbf{b}_j^*) \right] f_{G_n}(\mathbf{x}) \\ &\quad + \sum_{j:|\mathcal{V}_j|>1} \sum_{i \in \mathcal{V}_j} \exp(c_i^n) \left[E(\mathbf{x}; A_i^n, b_i^n) - E(\mathbf{x}; \mathbf{A}_j^*, \mathbf{b}_j^*) \right] f_{G_n}(\mathbf{x}) \\ &:= B_{n,1}(\mathbf{x}) + B_{n,2}(\mathbf{x}). \end{aligned}$$

By reusing the above techniques, we can decompose $B_{n,1}(\mathbf{x})$ as

$$\begin{aligned} B_{n,1}(\mathbf{x}) &= \sum_{j:|\mathcal{V}_j|=1} \sum_{i \in \mathcal{V}_j} \frac{\exp(c_i^n)}{\alpha!} \sum_{|\alpha|=1} (\Delta A_{ij}^n)^{\alpha_1} (\Delta b_{ij}^n)^{\alpha_2} \cdot \frac{\partial^{2|\alpha_1|+|\alpha_2|} E}{\partial b^{\tau(\alpha_1, \alpha_2)}}(\mathbf{x}; \mathbf{A}_j^*, \mathbf{b}_j^*) f_{G_n}(\mathbf{x}) \\ &\quad + R_{n,3}(\mathbf{x}) \\ &= \sum_{j:|\mathcal{V}_j|=1} \sum_{|\ell_2|=1}^2 T_{n,j,\ell_2} \cdot \frac{\partial^{|\ell_2|} E}{\partial b^{\ell_2}}(\mathbf{x}; \mathbf{A}_j^*, \mathbf{b}_j^*) f_{G_n}(\mathbf{x}) + R_{n,3}(\mathbf{x}), \end{aligned}$$

where we denote

$$T_{n,j,\ell_2} := \sum_{i \in \mathcal{V}_j} \sum_{\tau(\alpha_1, \alpha_2)=\ell_2} \frac{\exp(c_i^n)}{\alpha!} (\Delta A_{ij}^n)^{\alpha_1} (\Delta b_{ij}^n)^{\alpha_2}$$

for any $j \in [N^*]$ and $\ell_2 \neq \mathbf{0}_d$. Meanwhile, $R_{n,3}(\mathbf{x})$ is a Taylor remainder such that $R_{n,3}(\mathbf{x})/\mathcal{L}_{1n} \rightarrow 0$ as $n \rightarrow \infty$. Similarly, we also have that

$$B_{n,2}(\mathbf{x}) = \sum_{j:|\mathcal{V}_j|>1} \sum_{|\ell_2|=1}^{2\bar{r}_j} T_{n,j,\ell_2} \cdot \frac{\partial^{|\ell_2|} E}{\partial b^{\ell_2}}(\mathbf{x}; \mathbf{A}_j^*, \mathbf{b}_j^*) f_{G_n}(\mathbf{x}) + R_{n,4}(\mathbf{x}),$$

where $R_{n,4}(\mathbf{x})$ is a Taylor remainder such that $R_{n,4}(\mathbf{x})/\mathcal{L}_{1n} \rightarrow 0$ as $n \rightarrow \infty$.

Putting the above results together, we can decompose the term $Q_n(\mathbf{x})$ as

$$\begin{aligned} Q_n(\mathbf{x}) &= \sum_{j=1}^{N^*} \sum_{|\alpha_3|=0}^{\bar{r}_j} \sum_{|\ell_1|=0}^{2(\bar{r}_j-|\alpha_3|)} S_{n,j,\alpha_3,\ell_1} \cdot \frac{\partial^{|\ell_1|} E}{\partial b^{\ell_1}}(\mathbf{x}; \mathbf{A}_j^*, \mathbf{b}_j^*) \frac{\partial^{|\alpha_3|} h}{\partial \boldsymbol{\eta}^{\alpha_3}}(\mathbf{x}; \boldsymbol{\eta}_j^*) \\ &\quad - \sum_{j=1}^{N^*} \sum_{|\ell_2|=0}^{2\bar{r}_j} T_{n,j,\ell_2} \cdot \frac{\partial^{|\ell_2|} E}{\partial b^{\ell_2}}(\mathbf{x}; \mathbf{A}_j^*, \mathbf{b}_j^*) f_{G_n}(\mathbf{x}) + \sum_{i=1}^4 R_{n,i}(\mathbf{x}), \end{aligned} \tag{39}$$

where we define $S_{n,j,\mathbf{0}_q, \mathbf{0}_d} = T_{n,j,\mathbf{0}_d} = \sum_{i \in \mathcal{V}_j} \exp(c_i^n) - \exp(c_j^*)$ for any $j \in [N^*]$.

Step 2 - Non-vanishing coefficients. In this step, we prove by contradiction that at least one among ratios of the forms $S_{n,j,\alpha_3,\ell_1}/\mathcal{L}_{1n}$ and $T_{n,j,\ell_2}/\mathcal{L}_{1n}$ goes to zero as n tends to infinity. Assume that

$$\frac{S_{n,j,\alpha_3,\ell_1}}{\mathcal{L}_{1n}} \rightarrow 0, \quad \frac{T_{n,j,\ell_2}}{\mathcal{L}_{1n}} \rightarrow 0,$$

for any $j \in [N^*]$, $0 \leq |\alpha_3| \leq \bar{r}_j$, $0 \leq |\ell_1| \leq 2(\bar{r}_j - |\alpha_3|)$ and $0 \leq |\ell_2| \leq 2\bar{r}_j$.

First of all, it is worth noting that as $n \rightarrow \infty$,

$$\frac{1}{\mathcal{L}_{1n}} \sum_{j=1}^{N^*} \left| \sum_{i \in \mathcal{V}_j} \exp(c_i^n) - \exp(c_j^*) \right| = \sum_{j=1}^{N^*} \left| \frac{S_{n,j,\mathbf{0}_q,\mathbf{0}_d}}{\mathcal{L}_{1n}} \right| \rightarrow 0. \quad (40)$$

Now, let us consider indices $j \in [N^*]$ such that its corresponding Voronoi cell has only one element, i.e. $|\mathcal{V}_j| = 1$.

- When $\alpha_3 = e_{q,u} := (0, \dots, 0, \underbrace{1}_{u-th}, 0, \dots, 0) \in \mathbb{N}^q$ and $\ell_1 = \mathbf{0}_d$, we have $\frac{1}{\mathcal{L}_{1n}} \cdot \sum_{i \in \mathcal{V}_j} \exp(c_i^n) |(\Delta \boldsymbol{\eta}_{ij}^n)^{(u)}| = |S_{n,j,\alpha_3,\ell_1}| / \mathcal{L}_{1n} \rightarrow 0$ as $n \rightarrow \infty$. By taking the summation of the previous term with $u \in [q]$, we achieve that $\frac{1}{\mathcal{L}_{1n}} \sum_{i \in \mathcal{V}_j} \exp(c_i^n) \|\Delta \boldsymbol{\eta}_{ij}^n\|_1 \rightarrow 0$. Owing to the topological equivalence between norm-1 and norm-2, it follows that

$$\frac{1}{\mathcal{L}_{1n}} \sum_{i \in \mathcal{V}_j} \exp(c_i^n) \|\Delta \boldsymbol{\eta}_{ij}^n\| \rightarrow 0. \quad (41)$$

- When $\alpha_3 = \mathbf{0}_q$ and $\ell_1 = e_{d,u} := (0, \dots, 0, \underbrace{1}_{u-th}, 0, \dots, 0) \in \mathbb{N}^d$, by using the above arguments, we get that

$$\frac{1}{\mathcal{L}_{1n}} \sum_{i \in \mathcal{V}_j} \exp(c_i^n) \|\Delta \boldsymbol{b}_{ij}^n\| \rightarrow 0. \quad (42)$$

- When $\alpha_3 = \mathbf{0}_q$ and $\ell_1 = 2e_{d,u}$, it follows that

$$\frac{1}{\mathcal{L}_{1n}} \sum_{i \in \mathcal{V}_j} \exp(c_i^n) \|\Delta \boldsymbol{A}_{ij}^n\| \rightarrow 0. \quad (43)$$

Combine the limits in equations (41), (42) and (43), we obtain that

$$\frac{1}{\mathcal{L}_{1n}} \sum_{j:|\mathcal{V}_j|=1} \sum_{i \in \mathcal{V}_j} \exp(c_i^n) [\|\Delta \boldsymbol{A}_{ij}^n\| + \|\Delta \boldsymbol{b}_{ij}^n\| + \|\Delta \boldsymbol{\eta}_{ij}^n\|] \rightarrow 0, \quad (44)$$

as $n \rightarrow \infty$.

Next, we consider indices $j \in [N^*]$ such that its corresponding Voronoi cell has more than one element, i.e. $|\mathcal{V}_j| > 1$. When $\alpha_3 = 2e_{q,u}$ and $\ell_1 = \mathbf{0}_d$, we get $\frac{1}{\mathcal{L}_{1n}} \cdot \sum_{i \in \mathcal{V}_j} \exp(c_i^n) |(\Delta \boldsymbol{\eta}_{ij}^n)^{(u)}|^2 = |2S_{n,j,\alpha_3,\ell_1}| / \mathcal{L}_{1n} \rightarrow 0$ as $n \rightarrow \infty$. By taking the summation of the previous term with $u \in [q]$, we achieve that $\frac{1}{\mathcal{L}_{1n}} \sum_{i \in \mathcal{V}_j} \exp(c_i^n) \|\Delta \boldsymbol{\eta}_{ij}^n\|^2 \rightarrow 0$. This result indicates that

$$\frac{1}{\mathcal{L}_{1n}} \sum_{j:|\mathcal{V}_j|>1} \sum_{i \in \mathcal{V}_j} \exp(c_i^n) \|\Delta \boldsymbol{\eta}_{ij}^n\|^2 \rightarrow 0, \quad (45)$$

as $n \rightarrow \infty$. It follows from the limits in equations (40), (44), (45) and the formulation of \mathcal{L}_{1n} in equation (36) that

$$\frac{1}{\mathcal{L}_{1n}} \sum_{j:|\mathcal{V}_j|>1} \sum_{i \in \mathcal{V}_j} \exp(c_i^n) [\|\Delta \boldsymbol{A}_{ij}^n\|^{\bar{r}_j/2} + \|\Delta \boldsymbol{b}_{ij}^n\|^{\bar{r}_j}] \rightarrow 1.$$

The above limit suggests that there exists an index $j' : |\mathcal{V}_{j'}| > 1$ such that

$$\frac{1}{\mathcal{L}_{1n}} \sum_{i \in \mathcal{V}_{j'}} \exp(c_i^n) [\|\Delta A_{ij'}^n\|^{\bar{r}_{j'}/2} + \|\Delta b_{ij'}^n\|^{\bar{r}_{j'}}] \not\rightarrow 0. \quad (46)$$

Without loss of generality, we may assume that $j' = 1$.

Case 1. $\frac{1}{\mathcal{L}_{1n}} \sum_{i \in \mathcal{V}_1} \exp(c_i^n) [\|(\Delta A_{i1}^n)^{(uu)}\|_{u=1}^{\bar{r}_1/2} + \|\Delta b_{i1}^n\|^{\bar{r}_1}] \not\rightarrow 0$.

In this case, there exists some $u' \in [d]$ such that

$$\frac{1}{\mathcal{L}_{1n}} \sum_{i \in \mathcal{V}_1} \exp(c_i^n) [|(\Delta A_{i1}^n)^{(u'u')}|^{\bar{r}_1/2} + |(\Delta b_{i1}^n)^{(u')}|^{\bar{r}_1}] \not\rightarrow 0.$$

Again, we may assume WLOG that $u' = 1$ throughout Case 1, i.e.

$$\frac{1}{\mathcal{L}_{1n}} \sum_{i \in \mathcal{V}_1} \exp(c_i^n) [|(\Delta A_{i1}^n)^{(11)}|^{\bar{r}_1/2} + |(\Delta b_{i1}^n)^{(1)}|^{\bar{r}_1}] \not\rightarrow 0. \quad (47)$$

Next, let us consider the term

$$S_{n,1,\mathbf{0}_q,\ell_1} = \sum_{i \in \mathcal{V}_1} \sum_{\tau(\alpha_1, \alpha_2) = \ell_1} \frac{\exp(c_i^n)}{\alpha_1! \alpha_2!} (\Delta \mathbf{A}_{ij}^n)^{\alpha_1} (\Delta \mathbf{b}_{ij}^n)^{\alpha_2}, \quad (48)$$

where $\ell_1 \in \mathcal{N}^d$ such that $\ell_1^{(u)} = 0$ for any $u = 2, 3, \dots, d$. Then, the constraint $\tau(\alpha_1, \alpha_2) = \ell_1$ holds iff $\alpha_1^{(u1)} = \alpha_1^{(1v)} = \alpha_1^{(uv)} = \alpha_2^{(u)}$ for all $u, v = 2, 3, \dots, d$. Thus, by assumption, we get

$$\frac{1}{\mathcal{L}_{1n}} \sum_{i \in \mathcal{V}_1} \sum_{2\alpha_1^{(11)} + \alpha_2^{(1)} = \ell_1^{(1)}} \frac{\exp(c_i^n)}{\alpha_1^{(11)}! \alpha_2^{(1)}!} (\Delta \mathbf{A}_{ij}^n)^{\alpha_1^{(11)}} (\Delta \mathbf{b}_{ij}^n)^{\alpha_2^{(1)}} = \frac{S_{n,1,\mathbf{0}_q,\ell_1}}{\mathcal{L}_{1n}} \rightarrow 0. \quad (49)$$

By dividing the left hand side of equation (49) by that of equation (47), we get

$$\frac{\sum_{i \in \mathcal{V}_1} \sum_{2\alpha_1^{(11)} + \alpha_2^{(1)} = \ell_1^{(1)}} \frac{\exp(c_i^n)}{\alpha_1^{(11)}! \alpha_2^{(1)}!} (\Delta \mathbf{A}_{ij}^n)^{\alpha_1^{(11)}} (\Delta \mathbf{b}_{ij}^n)^{\alpha_2^{(1)}}}{\sum_{i \in \mathcal{V}_1} \exp(c_i^n) [|\Delta A_{i1}^n|^{(11)}|^{\bar{r}_1/2} + |(\Delta b_{i1}^n)^{(1)}|^{\bar{r}_1}]} \rightarrow 0. \quad (50)$$

Subsequently, we define $M_n := \max\{|\Delta A_{i1}^n|^{(11)}|^{1/2}, |(\Delta b_{i1}^n)^{(1)}| : i \in \mathcal{V}_1\}$ and $\pi_n = \max_{i \in \mathcal{V}_1} \exp(c_i^n)$. For any $i \in \mathcal{V}_1$, it is clear that the sequence of positive real numbers $(\exp(c_i^n)/\pi_n)$ is bounded, therefore, we can replace it by its subsequence that admits a non-negative limit denoted by $p_i^2 = \lim_{n \rightarrow \infty} \exp(c_i^n)/\pi_n$. In addition, let us denote $(\Delta A_{i1}^n)^{(11)}/M_n^2 \rightarrow \gamma_{1i}$ and $(\Delta b_{i1}^n)^{(1)}/M_n \rightarrow \gamma_{2i}$. Since $\exp(c_i^n) \geq \beta$ for some $\beta > 0$, the real numbers p_i will not vanish, and at least one of them is equal to 1. Analogously, at least one of the terms γ_{1i} and γ_{2i} is equal to either 1 or -1.

Note that $\sum_{i \in \mathcal{V}_1} \exp(c_i^n) (|\Delta A_{i1}^n|^{(11)}|^{\bar{r}_1/2} + |(\Delta b_{i1}^n)^{(1)}|^{\bar{r}_1}) / (\pi_n M_n^{\ell_1^{(1)}}) \not\rightarrow 0$ for all $\ell_1^{(1)} \in [\bar{r}_1]$. Thus, we are able to divide both the numerator and the denominator in equation (50) by $\pi_n M_n^{\ell_1^{(1)}}$ and let $n \rightarrow \infty$ in order to achieve the following system of polynomial equations:

$$\sum_{i \in \mathcal{V}_1} \sum_{2\alpha_1^{(11)} + \alpha_2^{(1)} = \ell_1^{(1)}} \frac{p_i^2 \gamma_{1i}^{\alpha_1^{(11)}} \gamma_{2i}^{\alpha_2^{(1)}}}{\alpha_1^{(11)}! \alpha_2^{(1)}!} = 0, \quad \ell_1^{(1)} \in [\bar{r}_1].$$

However, by the definition of \bar{r}_1 , the above system cannot admit any non-trivial solutions, which is a contradiction. Thus, Case 1 cannot happen.

Case 2. $\frac{1}{\mathcal{L}_{1n}} \sum_{i \in \mathcal{V}_1} \exp(c_i^n) \|((\Delta A_{i1}^n)^{(uv)})_{1 \leq u \neq v \leq d}\|^{\bar{r}_1/2} \not\rightarrow 0$.

In this case, there exist some indices u', v' such that $u' \neq v'$ and

$$\frac{1}{\mathcal{L}_{1n}} \cdot \sum_{i \in \mathcal{V}_1} \exp(c_i^n) |(\Delta A_{i1}^n)^{(u'v')}|^{\bar{r}_1/2} \not\rightarrow 0.$$

Recall that $|\mathcal{V}_1| > 1$, or equivalently, $|\mathcal{V}_1| \geq 2$, we have that $\bar{r}_1 \geq 4$. Therefore, the above equation leads to

$$\frac{1}{\mathcal{L}_{1n}} \cdot \sum_{i \in \mathcal{V}_1} \exp(c_i^n) |(\Delta A_{i1}^n)^{(u'v')}|^2 \not\rightarrow 0. \quad (51)$$

WLOG, we assume that $u' = 1$ and $v' = 2$ throughout Case 2. We continue to consider the coefficient $S_{n,1,\mathbf{0}_q,\ell_1}$ in equation (48) with $\ell_1 = (2, 2, 0, \dots, 0) \in \mathbb{N}^d$. By assumption, we have $S_{n,1,\mathbf{0}_q,\ell_1}/\mathcal{L}_{1n} \rightarrow 0$, which together with equation (51) imply that

$$\frac{\sum_{i \in \mathcal{V}_1} \sum_{\tau(\alpha_1, \alpha_2) = \ell_1} \frac{\exp(c_i^n)}{\alpha_1! \alpha_2!} (\Delta A_{i1}^n)^{\alpha_1} (\Delta b_{i1}^n)^{\alpha_2}}{\sum_{i \in \mathcal{V}_1} \exp(c_i^n) |(\Delta A_{i1}^n)^{(12)}|^2} \rightarrow 0. \quad (52)$$

Similarly, by combining the fact that case 1.1 does not hold and the result in equation (51), we get

$$\frac{\sum_{i \in \mathcal{V}_1} \exp(c_i^n) \left(\|((\Delta A_{i1}^n)^{(uu)})_{u=1}^d\|^{\bar{r}_1/2} + \|\Delta b_{i1}^n\|^{\bar{r}_1} \right)}{\sum_{i \in \mathcal{V}_1} \exp(c_i^n) |(\Delta A_{i1}^n)^{(12)}|^2} \rightarrow 0.$$

Since $\bar{r}_1 \geq 4$, the above limit indicates that any terms in equation (52) with $\alpha_1^{(uu)} > 0$ and $\alpha_2^{(u)} > 0$ for $u \in \{1, 2\}$ will vanish. Consequently, we deduce from equation (52) that

$$1 = \frac{\sum_{i \in \mathcal{V}_1} \exp(c_i^n) |(\Delta A_{i1}^n)^{(12)}|^2}{\sum_{i \in \mathcal{V}_1} \exp(c_i^n) |(\Delta A_{i1}^n)^{(12)}|^2} \rightarrow 0,$$

which is a contradiction. Thus, Case 2 cannot happen.

Collect the results from Case 1 and Case 2, we can conclude that the claim in equation (46), which is a contradiction. Therefore, at least one among ratios of the forms $S_{n,j,\alpha_3,\ell_1}/\mathcal{L}_{1n}$ and $T_{n,j,\ell_2}/\mathcal{L}_{1n}$ goes to zero as $n \rightarrow \infty$.

Step 3. Application of Fatou's lemma. In this step, we show that all the ratios $S_{n,j,\alpha_3,\ell_1}/\mathcal{L}_{1n}$ and $T_{n,j,\ell_2}/\mathcal{L}_{1n}$ go to zero as $n \rightarrow \infty$, which contradicts to the conclusion in Step 2. In particular, by denoting m_n as the maximum of the absolute values of those ratios. From the result of Step 2, it follows that $1/m_n \not\rightarrow \infty$.

Recall from the hypothesis in equation (35) that $\|f_{G_n} - f_{G_*}\|_{L_2(\mu)}/\mathcal{L}_{1n} \rightarrow 0$ as $n \rightarrow \infty$, which indicates that $\|f_{G_n} - f_{G_*}\|_{L^1(\mu)}/\mathcal{L}_{1n} \rightarrow 0$. Therefore, by applying the Fatou's lemma, we get that

$$0 = \lim_{n \rightarrow \infty} \frac{\|f_{G_n} - f_{G_*}\|_{L^1(\mu)}}{m_n \mathcal{L}_{1n}} \geq \int \liminf_{n \rightarrow \infty} \frac{|f_{G_n}(\mathbf{x}) - f_{G_*}(\mathbf{x})|}{m_n \mathcal{L}_{1n}} d\mu(\mathbf{x}) \geq 0.$$

This result implies that $\frac{1}{m_n \mathcal{L}_{1n}} \cdot [f_{G_n}(\mathbf{x}) - f_{G_*}(\mathbf{x})] \rightarrow 0$ as $n \rightarrow \infty$ for μ -almost surely x . Looking at the formulation of $Q_n(\mathbf{x})$ in equation (37), since the term $\left[\sum_{j=1}^{N^*} \exp(\mathbf{x}^\top \mathbf{A}_j^* \mathbf{x} + (\mathbf{b}_j^*)^\top \mathbf{x} + c_j^*) \right]$ is bounded, we deduce that the term $\frac{1}{m_n \mathcal{L}_{1n}} \cdot Q_n(\mathbf{x}) \rightarrow 0$ for μ -almost surely x .

Let us denote

$$\frac{S_{n,j,\alpha_3,\ell_1}}{m_n \mathcal{L}_{1n}} \rightarrow \phi_{j,\alpha_3,\ell_1}, \quad \frac{T_{n,j,\ell_2}}{m_n \mathcal{L}_{1n}} \rightarrow \varphi_{j,\ell_2},$$

with a note that at least one among them is non-zero. Then, from the decomposition of $Q_n(\mathbf{x})$ in equation (39), we have

$$\begin{aligned} & \sum_{j=1}^{N^*} \sum_{|\alpha_3|=0}^{\bar{r}_j} \sum_{|\ell_1|=0}^{2(\bar{r}_j-|\alpha_3|)} \phi_{j,\alpha_3,\ell_1} \cdot \frac{\partial^{|\ell_1|} E}{\partial b^{\ell_1}}(\mathbf{x}; \mathbf{A}_j^*, \mathbf{b}_j^*) \frac{\partial^{|\alpha_3|} h}{\partial \eta^{\alpha_3}}(\mathbf{x}; \boldsymbol{\eta}_j^*) \\ & \quad - \sum_{j=1}^{N^*} \sum_{|\ell_2|=0}^{2\bar{r}_j} \varphi_{j,\ell_2} \cdot \frac{\partial^{|\ell_2|} E}{\partial b^{\ell_2}}(\mathbf{x}; \mathbf{A}_j^*, \mathbf{b}_j^*) f_{G_*}(\mathbf{x}) = 0, \end{aligned}$$

for μ -almost surely x . Since the expert function h satisfies the condition in Definition 3.2, we obtain that $\phi_{j,\alpha_3,\ell_1} = \varphi_{j,\ell_2} = 0$ for all $j \in [N^*]$, $0 \leq |\alpha_3| \leq \bar{r}_j$, $0 \leq |\ell_1| \leq 2(\bar{r}_j - |\alpha_3|)$ and $0 \leq |\ell_2| \leq 2\bar{r}_j$. This result turns out to contradict the fact that at least one among them is different from zero. Hence, we achieve the inequality in equation (34).

Global part. It is worth noting that the inequality (34) suggests that there exists a positive constant ε' such that

$$\inf_{G \in \mathcal{G}_N(\Theta): \mathcal{L}_1(G, G_*) \leq \varepsilon'} \|f_G - f_{G_*}\|_{L_2(\mu)} / \mathcal{L}_1(G, G_*) > 0.$$

Therefore, it is sufficient to prove that

$$\inf_{G \in \mathcal{G}_N(\Theta): \mathcal{L}_1(G, G_*) > \varepsilon'} \|f_G - f_{G_*}\|_{L_2(\mu)} / \mathcal{L}_1(G, G_*) > 0. \quad (53)$$

Assume by contrary that the inequality (53) does not hold true, then we can find a sequence of mixing measures $G'_n \in \mathcal{G}_N(\Theta)$ such that $\mathcal{L}_1(G'_n, G_*) > \varepsilon'$ and

$$\lim_{n \rightarrow \infty} \frac{\|f_{G'_n} - f_{G_*}\|_{L_2(\mu)}}{\mathcal{L}_1(G'_n, G_*)} = 0,$$

which indicates that $\|f_{G'_n} - f_{G_*}\|_{L_2(\mu)} \rightarrow 0$ as $n \rightarrow \infty$. Recall that Θ is a compact set, therefore, we can replace the sequence G'_n by one of its subsequences that converges to a mixing measure $G' \in \mathcal{G}_N(\Omega)$. Since $\mathcal{L}_1(G'_n, G_*) > \varepsilon'$, we deduce that $\mathcal{L}_1(G', G_*) > \varepsilon'$.

Next, by invoking the Fatou's lemma, we have that

$$0 = \lim_{n \rightarrow \infty} \|f_{G'_n} - f_{G_*}\|_{L_2(\mu)}^2 \geq \int \liminf_{n \rightarrow \infty} \left| f_{G'_n}(\mathbf{x}) - f_{G_*}(\mathbf{x}) \right|^2 d\mu(\mathbf{x}).$$

Thus, we get that $f_{G'}(\mathbf{x}) = f_{G_*}(\mathbf{x})$ for μ -almost surely x . From Proposition E.1, we deduce that $G' \equiv G_*$. Consequently, it follows that $\mathcal{L}_1(G', G_*) = 0$, contradicting the fact that $\mathcal{L}_1(G', G_*) > \varepsilon' > 0$. Hence, the proof is completed.

D.3 Proof of Theorem C.1

In this proof, we first introduce the following lemma which will be used for our subsequent main proof of Theorem C.1.

Lemma D.2. *Suppose that the following holds for any $r \geq 1$:*

$$\lim_{\varepsilon \rightarrow 0} \inf_{G \in \mathcal{G}_N(\Theta) : \mathcal{L}_{2,r}(G, G_*) \leq \varepsilon} \frac{\|f_G - f_{G_*}\|_{L_2(\mu)}}{\mathcal{L}_{2,r}(G, G_*)} = 0. \quad (54)$$

Then, we achieve that for any $r \geq 1$:

$$\inf_{\bar{G}_n \in \mathcal{G}_N(\Theta)} \sup_{G \in \mathcal{G}_N(\Theta) \setminus \mathcal{G}_{N^*-1}(\Theta)} \mathbb{E}_{f_G} [\mathcal{L}_{2,r}(\bar{G}_n, G)] \gtrsim n^{-1/2}, \quad (55)$$

where \mathbb{E}_{f_G} indicates the expectation taken w.r.t the product measure with f_G^n .

Proof of Lemma D.2. Firstly, note that from the Gaussian assumption on the noise variables, we obtain that $Y_i | X_i \sim \mathcal{N}(f_{G_*}(\mathbf{x}_i), \sigma^2)$ for all $i \in [n]$. Next, it follows from the assumption in equation (54) that for sufficiently small $\varepsilon > 0$ and a fixed constant $C_1 > 0$ which we will choose later, there exists a mixing measure $G'_* \in \mathcal{G}_N(\Theta)$ such that $\mathcal{L}_{2,r}(G'_*, G_*) = 2\varepsilon$ and $\|f_{G'_*} - f_{G_*}\|_{L_2(\mu)} \leq C_1\varepsilon$. According to Le Cam's lemma [41], since the Voronoi loss function $\mathcal{L}_{2,r}$ satisfies the weak triangle inequality, we get that

$$\begin{aligned} & \inf_{\bar{G}_n \in \mathcal{G}_N(\Theta)} \sup_{G \in \mathcal{G}_N(\Theta) \setminus \mathcal{G}_{N^*-1}(\Theta)} \mathbb{E}_{f_G} [\mathcal{L}_{2,r}(\bar{G}_n, G)] \\ & \gtrsim \frac{\mathcal{L}_{2,r}(G'_*, G_*)}{8} \exp(-n \mathbb{E}_{X \sim \mu} [\text{KL}(\mathcal{N}(f_{G'_*}(\mathbf{x}), \sigma^2), \mathcal{N}(f_{G_*}(\mathbf{x}), \sigma^2))]) \\ & \gtrsim \varepsilon \cdot \exp(-n \|f_{G'_*} - f_{G_*}\|_{L_2(\mu)}^2), \\ & \gtrsim \varepsilon \cdot \exp(-C_1 n \varepsilon^2), \end{aligned} \quad (56)$$

where the second inequality is due to the fact that

$$\text{KL}(\mathcal{N}(f_{G'_*}(\mathbf{x}), \sigma^2), \mathcal{N}(f_{G_*}(\mathbf{x}), \sigma^2)) = \frac{(f_{G'_*}(\mathbf{x}) - f_{G_*}(\mathbf{x}))^2}{2\sigma^2}.$$

By choosing $\varepsilon = n^{-1/2}$, we obtain that $\varepsilon \cdot \exp(-C_1 n \varepsilon^2) = n^{-1/2} \exp(-C_1)$. As a consequence, we achieve the desired minimax lower bound in equation (55). \square

Given the result of Lemma D.2, it suffices to prove that the following limit holds true for any $r \geq 1$:

$$\lim_{\varepsilon \rightarrow 0} \inf_{G \in \mathcal{G}_N(\Theta) : \mathcal{L}_{2,r}(G, G_*) \leq \varepsilon} \frac{\|f_G - f_{G_*}\|_{L_2(\mu)}}{\mathcal{L}_{2,r}(G, G_*)} = 0. \quad (57)$$

To this end, we will construct a sequence of mixing measures (G_n) such that both $\mathcal{L}_{2,r}(G_n, G_*) \rightarrow 0$ and

$$\frac{\|f_{G_n} - f_{G_*}\|_{L_2(\mu)}}{\mathcal{L}_{2,r}(G_n, G_*)} \rightarrow 0,$$

as $n \rightarrow \infty$. In particular, we consider the sequence $G_n = \sum_{i=1}^{N^*+1} \exp(c_i^n) \delta_{(A_i^n, b_i^n, \beta_{1i}^n, \beta_{0i}^n)}$, where

- $\exp(c_1^n) = \exp(c_2^n) = \frac{1}{2} \exp(c_1^*) + \frac{1}{2n^{r+1}}$ and $\exp(c_i^n) = \exp(c_{i-1}^n)$ for any $3 \leq i \leq N^* + 1$;
- $A_1^n = A_2^n = A_1^*$ and $A_i^n = A_{i-1}^*$ for any $3 \leq i \leq N^* + 1$;
- $b_1^n = b_2^n = b_1^*$ and $b_i^n = b_{i-1}^*$ for any $3 \leq i \leq N^* + 1$;
- $\beta_{11}^n = \beta_{12}^n = \beta_{11}^*$ and $\beta_{1i}^n = \beta_{1(i-1)}^*$ for any $3 \leq i \leq N^* + 1$;
- $\beta_{01}^n = \beta_{01}^* + \frac{1}{n}$, $\beta_{02}^n = \beta_{01}^* - \frac{1}{n}$ and $\beta_{0i}^n = \beta_{0(i-1)}^*$ for any $3 \leq i \leq N^* + 1$.

Consequently, the loss function $\mathcal{L}_{2,r}(G_n, G_*)$ turns into

$$\mathcal{L}_{2,r}(G_n, G_*) = \frac{1}{n^{r+1}} + \left[\exp(c_1^*) + \frac{1}{n^{r+1}} \right] \cdot \frac{1}{n^r} = \mathcal{O}(n^{-r}). \quad (58)$$

which suggests that $\mathcal{L}_{2,r}(G_n, G_*) \rightarrow 0$ as $n \rightarrow \infty$.

Now, we prove that $\|f_{G_n} - f_{G_*}\|_{L_2(\mu)} / \mathcal{L}_{2,r}(G_n, G_*) \rightarrow 0$. For that purpose, let us consider

$$Q_n(\mathbf{x}) := \left[\sum_{j=1}^{N^*} \exp(\mathbf{x}^\top A_j^* \mathbf{x} + (b_j^*)^\top \mathbf{x}) \right] \cdot [f_{G_n}(\mathbf{x}) - f_{G_*}(\mathbf{x})].$$

Then, we decompose $Q_n(\mathbf{x})$ as $Q_n(\mathbf{x}) = A_n(\mathbf{x}) - B_n(\mathbf{x}) + C_n(\mathbf{x})$ where we define

$$\begin{aligned} A_n(\mathbf{x}) &= \sum_{j=1}^{N^*} \sum_{i \in \mathcal{V}_j} \exp(c_i^n) \left[\exp(\mathbf{x}^\top A_i^n \mathbf{x} + (b_i^n)^\top \mathbf{x}) ((\beta_{1i}^n)^\top \mathbf{x} + \beta_{0i}^n) \right. \\ &\quad \left. - \exp(\mathbf{x}^\top A_j^* \mathbf{x} + (b_j^*)^\top \mathbf{x}) ((\beta_{1j}^*)^\top \mathbf{x} + \beta_{0j}^*) \right], \\ B_n(\mathbf{x}) &= \sum_{j=1}^{N^*} \sum_{i \in \mathcal{V}_j} \exp(c_i^n) \left[\exp(\mathbf{x}^\top A_i^n \mathbf{x} + (b_i^n)^\top \mathbf{x}) - \exp(\mathbf{x}^\top A_j^* \mathbf{x} + (b_j^*)^\top \mathbf{x}) \right] f_{G_n}(\mathbf{x}), \\ C_n(\mathbf{x}) &= \sum_{j=1}^{N^*} \left(\sum_{i \in \mathcal{V}_j} \exp(c_i^n) - \exp(c_j^*) \right) \left[\exp(\mathbf{x}^\top A_j^* \mathbf{x} + (b_j^*)^\top \mathbf{x}) ((\beta_{1j}^*)^\top \mathbf{x} + \beta_{0j}^*) \right. \\ &\quad \left. - \exp(\mathbf{x}^\top A_j^* \mathbf{x} + (b_j^*)^\top \mathbf{x}) f_{G_n}(\mathbf{x}) \right]. \end{aligned}$$

From the definitions of A_i^n , b_i^n , β_{1i}^n and β_{0i}^n , we can rewrite $A_n(\mathbf{x})$ as follows:

$$\begin{aligned} A_n(\mathbf{x}) &= \frac{1}{2} \exp(c_1^n) \exp(\mathbf{x}^\top A_1^* \mathbf{x} + (b_1^*)^\top \mathbf{x}) [(\beta_{01}^n - \beta_{01}^*) + (\beta_{02}^n - \beta_{01}^*)] \\ &= \frac{1}{2} \exp(c_1^n) \exp(\mathbf{x}^\top A_1^* \mathbf{x} + (b_1^*)^\top \mathbf{x}) \left[\frac{1}{n} - \frac{1}{n} \right] = 0. \end{aligned}$$

Moreover, we can verify that $B_n(\mathbf{x}) = 0$. Next, we have

$$\begin{aligned} C_n(\mathbf{x}) &= \left(\sum_{i=1}^2 \exp(c_i^n) - \exp(c_1^*) \right) \exp(\mathbf{x}^\top A_1^* \mathbf{x} + (b_1^*)^\top \mathbf{x}) \left[((\beta_{11}^*)^\top \mathbf{x} + \beta_{01}^*) - f_{G_n}(\mathbf{x}) \right] \\ &= \frac{1}{n^{r+1}} \cdot \exp(\mathbf{x}^\top A_1^* \mathbf{x} + (b_1^*)^\top \mathbf{x}) \left[((\beta_{11}^*)^\top \mathbf{x} + \beta_{01}^*) - f_{G_n}(\mathbf{x}) \right] \\ &\leq \mathcal{O}(n^{-(r+1)}), \end{aligned}$$

which leads to the fact that $C_n(\mathbf{x})/\mathcal{L}_{2,r}(G_n, G_*) \rightarrow 0$ as $n \rightarrow \infty$.

As a result, $Q_n(\mathbf{x})/\mathcal{L}_{2,r}(G_n, G_*) \rightarrow 0$ for μ -almost surely x . Since the term $\sum_{j=1}^{N^*} \exp(\mathbf{x}^\top \mathbf{A}_j^* \mathbf{x} + (\mathbf{b}_j^*)^\top \mathbf{x})$ is bounded, we deduce that $[f_{G_n}(\mathbf{x}) - f_{G_*}(\mathbf{x})]/\mathcal{L}_{2,r}(G_n, G_*) \rightarrow 0$ for μ -almost surely x . This result indicates that $\|f_{G_n} - f_{G_*}\|_{L_2(\mu)}/\mathcal{L}_{2,r}(G_n, G_*) \rightarrow 0$ as $n \rightarrow \infty$. Hence, we achieve the claim (57) and complete the proof.

D.4 Proof of Theorem B.1

The proof of Theorem B.1 can be done in a similar fashion to that of Theorem 3.1 in Appendix D.1.

D.5 Proof of Theorem B.3

Our goal is also to demonstrate the following inequality:

$$\inf_{G \in \mathcal{G}_N(\Theta)} \|\tilde{f}_G - \tilde{f}_{G_*}\|_{L_2(\mu)}/\mathcal{L}_3(G, G_*) > 0. \quad (59)$$

For that purpose, we divide the proof of the above inequality into local and global parts in the sequel. Here, we only present the proof of the local part, while that of the global part can be done using the same arguments as in Appendix D.2.

Local part: In this part, we demonstrate that

$$\lim_{\varepsilon \rightarrow 0} \inf_{G \in \mathcal{G}_N(\Theta): \mathcal{L}_3(G, G_*) \leq \varepsilon} \|\tilde{f}_G - \tilde{f}_{G_*}\|_{L_2(\mu)}/\mathcal{L}_3(G, G_*) > 0. \quad (60)$$

Assume by contrary that the above claim is not true, then there exists a sequence of mixing measures $G_n = \sum_{i=1}^{N^*} \exp(c_i^n) \delta_{(\mathbf{A}_i^n, \boldsymbol{\eta}_i^n)}$ in $\mathcal{G}_N(\Theta)$ such that $\mathcal{L}_{3n} := \mathcal{L}_3(G_n, G_*) \rightarrow 0$ and

$$\|\tilde{f}_{G_n} - \tilde{f}_{G_*}\|_{L_2(\mu)}/\mathcal{L}_{1n} \rightarrow 0, \quad (61)$$

as $n \rightarrow \infty$. Let us denote by $\mathcal{V}_j^n := \mathcal{V}_j(G_n)$ a Voronoi cell of G_n generated by the j -th components of G_* . Since our arguments are asymptotic, we may assume that those Voronoi cells do not depend on the sample size, i.e. $\mathcal{V}_j = \mathcal{V}_j^n$. Thus, the Voronoi loss \mathcal{L}_{3n} can be represented as

$$\begin{aligned} \mathcal{L}_{3n} := & \sum_{j:|\mathcal{V}_j|>1} \sum_{i \in \mathcal{V}_j} \exp(c_i^n) \left[\|\Delta \mathbf{A}_{ij}^n\|^2 + \|\Delta \boldsymbol{\eta}_{ij}^n\|^2 \right] \\ & + \sum_{j:|\mathcal{V}_j|=1} \sum_{i \in \mathcal{V}_j} \exp(c_i^n) \left[\|\Delta \mathbf{A}_{ij}^n\| + \|\Delta \boldsymbol{\eta}_{ij}^n\| \right] + \sum_{j=1}^{N^*} \left| \sum_{i \in \mathcal{V}_j} \exp(c_i^n) - \exp(c_j^*) \right|, \end{aligned} \quad (62)$$

where we denote $\Delta \mathbf{A}_{ij}^n := \mathbf{A}_i^n - \mathbf{A}_j^*$ and $\Delta \boldsymbol{\eta}_{ij}^n := \boldsymbol{\eta}_i^n - \boldsymbol{\eta}_j^*$.

Since $\mathcal{L}_{3n} \rightarrow 0$, we get that $(\mathbf{A}_i^n, \boldsymbol{\eta}_i^n) \rightarrow (\mathbf{A}_j^*, \boldsymbol{\eta}_j^*)$ and $\sum_{i \in \mathcal{V}_j} \exp(c_i^n) \rightarrow \exp(c_j^*)$ as $n \rightarrow \infty$ for any $i \in \mathcal{V}_j$ and $j \in [N^*]$. Now, we divide the proof of local part into three steps as follows:

Step 1 - Taylor expansion. By abuse of notations, we sometimes tailor notations defined in Appendix D.2 to the setting of this proof. In this step, we would like to decompose the quantity

$$Q_n(\mathbf{x}) := \left[\sum_{j=1}^{N^*} \exp(\mathbf{x}^\top \mathbf{A}_j^* \mathbf{x} + c_j^*) \right] \cdot [\tilde{f}_{G_n}(\mathbf{x}) - \tilde{f}_{G_*}(\mathbf{x})] \quad (63)$$

into a combination of linearly independent elements using Taylor expansion. By using the same arguments for deriving equation (38), we get that $Q_n(\mathbf{x}) = A_n(\mathbf{x}) - B_n(\mathbf{x}) + C_n(\mathbf{x})$, where

$$\begin{aligned} A_n(\mathbf{x}) &:= \sum_{j=1}^{N^*} \sum_{i \in \mathcal{V}_j} \exp(c_i^n) \left[\exp(\mathbf{x}^\top A_i^n \mathbf{x}) h(\mathbf{x}; \eta_i^n) - \exp(\mathbf{x}^\top \mathbf{A}_j^* \mathbf{x}) h(\mathbf{x}; \boldsymbol{\eta}_j^*) \right], \\ B_n(\mathbf{x}) &:= \sum_{j=1}^{N^*} \sum_{i \in \mathcal{V}_j} \exp(c_i^n) \left[\exp(\mathbf{x}^\top A_i^n \mathbf{x}) - \exp(\mathbf{x}^\top \mathbf{A}_j^* \mathbf{x}) \right] \tilde{f}_{G_n}(\mathbf{x}), \\ C_n(\mathbf{x}) &:= \sum_{j=1}^{N^*} \left(\sum_{i \in \mathcal{V}_j} \exp(c_i^n) - \exp(c_j^*) \right) \left[\exp(\mathbf{x}^\top \mathbf{A}_j^* \mathbf{x}) h(\mathbf{x}; \boldsymbol{\eta}_j^*) - \exp(\mathbf{x}^\top \mathbf{A}_j^* \mathbf{x}) \tilde{f}_{G_n}(\mathbf{x}) \right]. \end{aligned}$$

Decomposition of A_n . Let us denote $E(\mathbf{x}; A) := \exp(\mathbf{x}^\top A \mathbf{x})$, then A_n can be separated into two terms as follows:

$$\begin{aligned} A_n(\mathbf{x}) &:= \sum_{j:|\mathcal{V}_j|=1} \sum_{i \in \mathcal{V}_j} \exp(c_i^n) \left[E(\mathbf{x}; A_i^n) h(\mathbf{x}; \eta_i^n) - E(\mathbf{x}; \mathbf{A}_j^*) h(\mathbf{x}; \boldsymbol{\eta}_j^*) \right] \\ &\quad + \sum_{j:|\mathcal{V}_j|>1} \sum_{i \in \mathcal{V}_j} \exp(c_i^n) \left[E(\mathbf{x}; A_i^n) h(\mathbf{x}; \eta_i^n) - E(\mathbf{x}; \mathbf{A}_j^*) h(\mathbf{x}; \boldsymbol{\eta}_j^*) \right] \\ &:= A_{n,1}(\mathbf{x}) + A_{n,2}(\mathbf{x}). \end{aligned}$$

By means of the first-order Taylor expansion, we have

$$\begin{aligned} A_{n,1}(\mathbf{x}) &= \sum_{j:|\mathcal{V}_j|=1} \sum_{i \in \mathcal{V}_j} \frac{\exp(c_i^n)}{\alpha!} \sum_{|\alpha|=1} (\Delta A_{ij}^n)^{\alpha_1} (\Delta \boldsymbol{\eta}_{ij}^n)^{\alpha_2} \frac{\partial^{|\alpha_1|} E}{\partial A^{\alpha_1}}(\mathbf{x}; \mathbf{A}_j^*) \frac{\partial^{|\alpha_2|} h}{\partial \boldsymbol{\eta}^{\alpha_2}}(\mathbf{x}; \boldsymbol{\eta}_j^*) + R_{n,1}(\mathbf{x}) \\ &= \sum_{j:|\mathcal{V}_j|=1} \sum_{|\alpha_1|+|\alpha_2|=1} S_{n,j,\alpha_1,\alpha_2} \frac{\partial^{|\alpha_1|} E}{\partial A^{\alpha_1}}(\mathbf{x}; \mathbf{A}_j^*) \frac{\partial^{|\alpha_2|} h}{\partial \boldsymbol{\eta}^{\alpha_2}}(\mathbf{x}; \boldsymbol{\eta}_j^*) + R_{n,1}(\mathbf{x}), \end{aligned}$$

where $R_{n,1}(\mathbf{x})$ is a Taylor remainder such that $R_{n,1}(\mathbf{x})/\mathcal{L}_{3n} \rightarrow 0$ as $n \rightarrow \infty$, and

$$S_{n,j,\alpha_1,\alpha_2} := \sum_{i \in \mathcal{V}_j} \frac{\exp(c_i^n)}{\alpha!} (\Delta A_{ij}^n)^{\alpha_1} (\Delta \boldsymbol{\eta}_{ij}^n)^{\alpha_2}.$$

On the other hand, by applying the second-order Taylor expansion, we get that

$$A_{n,2}(\mathbf{x}) = \sum_{j:|\mathcal{V}_j|>1} \sum_{1 \leq |\alpha_1|+|\alpha_2| \leq 2} S_{n,j,\alpha_1,\alpha_2} \frac{\partial^{|\alpha_1|} E}{\partial A^{\alpha_1}}(\mathbf{x}; \mathbf{A}_j^*) \frac{\partial^{|\alpha_2|} h}{\partial \boldsymbol{\eta}^{\alpha_2}}(\mathbf{x}; \boldsymbol{\eta}_j^*) + R_{n,2}(\mathbf{x}),$$

in which $R_{n,2}(\mathbf{x})$ is a Taylor remainder such that $R_{n,2}(\mathbf{x})/\mathcal{L}_{3n} \rightarrow 0$ as $n \rightarrow \infty$.

Decomposition of B_n . Recall that we have

$$\begin{aligned} B_n(\mathbf{x}) &= \sum_{j:|\mathcal{V}_j|=1} \sum_{i \in \mathcal{V}_j} \exp(c_i^n) \left[E(\mathbf{x}; A_i^n) - E(\mathbf{x}; \mathbf{A}_j^*) \right] \tilde{f}_{G_n}(\mathbf{x}) \\ &\quad + \sum_{j:|\mathcal{V}_j|>1} \sum_{i \in \mathcal{V}_j} \exp(c_i^n) \left[E(\mathbf{x}; A_i^n) - E(\mathbf{x}; \mathbf{A}_j^*) \right] \tilde{f}_{G_n}(\mathbf{x}) \\ &:= B_{n,1}(\mathbf{x}) + B_{n,2}(\mathbf{x}). \end{aligned}$$

By invoking first-order and second-order Taylor expansions to $B_{n,1}(\mathbf{x})$ and $B_{n,2}(\mathbf{x})$, it follows that

$$\begin{aligned} B_{n,1}(\mathbf{x}) &= \sum_{j:|\mathcal{V}_j|=1} \sum_{|\ell|=1} T_{n,j,\ell} \cdot \frac{\partial^{|\ell|} E}{\partial A^\ell}(\mathbf{x}; \mathbf{A}_j^*) \tilde{f}_{G_n}(\mathbf{x}) + R_{n,3}(\mathbf{x}), \\ B_{n,2}(\mathbf{x}) &= \sum_{j:|\mathcal{V}_j|>1} \sum_{1 \leq |\ell| \leq 2} T_{n,j,\ell} \cdot \frac{\partial^{|\ell|} E}{\partial A^\ell}(\mathbf{x}; \mathbf{A}_j^*) \tilde{f}_{G_n}(\mathbf{x}) + R_{n,4}(\mathbf{x}), \end{aligned}$$

where we define

$$T_{n,j,\ell} := \sum_{i \in \mathcal{V}_j} \frac{\exp(c_i^n)}{\ell!} (\Delta \mathbf{A}_{ij}^n)^\ell.$$

Additionally, $R_{n,3}(\mathbf{x})$ and $R_{n,4}(\mathbf{x})$ are Taylor remainders such that $R_{n,3}(\mathbf{x})/\mathcal{L}_{3n} \rightarrow 0$ and $R_{n,4}(\mathbf{x})/\mathcal{L}_{3n} \rightarrow 0$ as $n \rightarrow \infty$.

Collect the above results together, we can represent $Q_n(\mathbf{x})$ as

$$\begin{aligned} Q_n(\mathbf{x}) &= \sum_{j=1}^{N^*} \sum_{0 \leq |\alpha_1|+|\alpha_2| \leq 2} S_{n,j,\alpha_1,\alpha_2} \frac{\partial^{|\alpha_1|} E}{\partial A^{\alpha_1}}(\mathbf{x}; \mathbf{A}_j^*) \frac{\partial^{|\alpha_2|} h}{\partial \boldsymbol{\eta}^{\alpha_2}}(\mathbf{x}; \boldsymbol{\eta}_j^*), \\ &\quad - \sum_{j=1}^{N^*} \sum_{0 \leq |\ell| \leq 2} T_{n,j,\ell} \cdot \frac{\partial^{|\ell|} E}{\partial A^\ell}(\mathbf{x}; \mathbf{A}_j^*) \tilde{f}_{G_n}(\mathbf{x}) + \sum_{i=1}^4 R_{n,i}(\mathbf{x}), \end{aligned} \quad (64)$$

where we define $S_{n,j,\mathbf{0}_{d \times d},\mathbf{0}_q} = T_{n,j,\mathbf{0}_{d \times d}} = \sum_{i \in \mathcal{V}_j} \exp(c_i^n) - \exp(c_j^*)$ for any $j \in [N^*]$.

Step 2 - Non-vanishing coefficients. In this step, we demonstrate that at least one among ratios of the forms $S_{n,j,\alpha_1,\alpha_2}/\mathcal{L}_{3n}$ and $T_{n,j,\ell}/\mathcal{L}_{3n}$ goes to zero as n tends to infinity. Indeed, assume by contrary that

$$\frac{S_{n,j,\alpha_1,\alpha_2}}{\mathcal{L}_{3n}} \rightarrow 0, \quad \frac{T_{n,j,\ell}}{\mathcal{L}_{3n}} \rightarrow 0,$$

for any $j \in [N^*]$, $0 \leq |\alpha_1|, |\alpha_2|, |\ell| \leq 2$. Then, we get

$$\frac{1}{\mathcal{L}_{3n}} \sum_{j=1}^{N^*} \left| \sum_{i \in \mathcal{V}_j} \exp(c_i^n) - \exp(c_j^*) \right| = \sum_{j=1}^{N^*} \left| \frac{S_{n,j,\mathbf{0}_{d \times d},\mathbf{0}_q}}{\mathcal{L}_{3n}} \right| \rightarrow 0. \quad (65)$$

Now, we consider indices $j \in [N^*]$ such that its corresponding Voronoi cell has only one element, i.e. $|\mathcal{V}_j| = 1$.

- For arbitrary $u, v \in [d]$, let $\alpha_1 \in \mathbb{N}^{d \times d}$ and $\alpha_2 = \mathbf{0}_q$ such that $\alpha_1^{(uv)} = 1$ while other entries equal to zero. Then, we have $\frac{1}{\mathcal{L}_{3n}} \cdot \sum_{i \in \mathcal{V}_j} \exp(c_i^n) |(\Delta \mathbf{A}_{ij}^n)^{(uv)}| = |S_{n,j,\alpha_1,\alpha_2}|/\mathcal{L}_{3n} \rightarrow 0$ as $n \rightarrow \infty$. By taking the summation of the previous term with $u, v \in [d]$, we achieve that $\frac{1}{\mathcal{L}_{3n}} \sum_{i \in \mathcal{V}_j} \exp(c_i^n) \|\Delta \mathbf{A}_{ij}^n\|_1 \rightarrow 0$. Owing to the topological equivalence between norm-1 and norm-2, it follows that

$$\frac{1}{\mathcal{L}_{3n}} \sum_{i \in \mathcal{V}_j} \exp(c_i^n) \|\Delta \mathbf{A}_{ij}^n\| \rightarrow 0. \quad (66)$$

- For arbitrary $u \in [d]$, let $\alpha_1 = \mathbf{0}_{d \times d}$ and $\alpha_2 \in \mathbb{N}^q$ such that $\alpha_2^{(u)} = 1$ while other entries equal to zero. Then, we get $\frac{1}{\mathcal{L}_{3n}} \cdot \sum_{i \in \mathcal{V}_j} \exp(c_i^n) |(\Delta \boldsymbol{\eta}_{ij}^n)^{(u)}| = |S_{n,j,\alpha_3,\ell_1}| / \mathcal{L}_{3n} \rightarrow 0$ as $n \rightarrow \infty$. By taking the summation of the previous term with $u \in [q]$, we achieve that $\frac{1}{\mathcal{L}_{3n}} \sum_{i \in \mathcal{V}_j} \exp(c_i^n) \|\Delta \boldsymbol{\eta}_{ij}^n\|_1 \rightarrow 0$, or equivalently,

$$\frac{1}{\mathcal{L}_{3n}} \sum_{i \in \mathcal{V}_j} \exp(c_i^n) \|\Delta \boldsymbol{\eta}_{ij}^n\| \rightarrow 0. \quad (67)$$

Combine the limits in equations (66) and (67), we obtain that

$$\frac{1}{\mathcal{L}_{3n}} \sum_{j:|\mathcal{V}_j|=1} \sum_{i \in \mathcal{V}_j} \exp(c_i^n) [\|\Delta \mathbf{A}_{ij}^n\| + \|\Delta \boldsymbol{\eta}_{ij}^n\|] \rightarrow 0, \quad (68)$$

as $n \rightarrow \infty$.

Next, we consider indices $j \in [N^*]$ such that its corresponding Voronoi cell has more than one element, i.e. $|\mathcal{V}_j| > 1$.

- For arbitrary $u, v \in [d]$, let $\alpha_1 \in \mathbb{N}^{d \times d}$ and $\alpha_2 = \mathbf{0}_q$ such that $\alpha_1^{(uv)} = 2$ while other entries equal to zero. Then, we have $\frac{1}{\mathcal{L}_{3n}} \cdot \sum_{i \in \mathcal{V}_j} \exp(c_i^n) |(\Delta \mathbf{A}_{ij}^n)^{(uv)}|^2 = |S_{n,j,\alpha_1,\alpha_2}| / \mathcal{L}_{3n} \rightarrow 0$ as $n \rightarrow \infty$. By taking the summation of the previous term with $u, v \in [d]$, we achieve that

$$\frac{1}{\mathcal{L}_{3n}} \sum_{i \in \mathcal{V}_j} \exp(c_i^n) \|\Delta \mathbf{A}_{ij}^n\|^2 \rightarrow 0. \quad (69)$$

- For arbitrary $u \in [d]$, let $\alpha_1 = \mathbf{0}_{d \times d}$ and $\alpha_2 \in \mathbb{N}^q$ such that $\alpha_2^{(u)} = 2$ while other entries equal to zero. Then, we get $\frac{1}{\mathcal{L}_{3n}} \cdot \sum_{i \in \mathcal{V}_j} \exp(c_i^n) |(\Delta \boldsymbol{\eta}_{ij}^n)^{(u)}|^2 = |S_{n,j,\alpha_3,\ell_1}| / \mathcal{L}_{3n} \rightarrow 0$ as $n \rightarrow \infty$. By taking the summation of the previous term with $u \in [q]$, we achieve that

$$\frac{1}{\mathcal{L}_{3n}} \sum_{i \in \mathcal{V}_j} \exp(c_i^n) \|\Delta \boldsymbol{\eta}_{ij}^n\|^2 \rightarrow 0. \quad (70)$$

Putting the limits in equations (66) and (67), we have

$$\frac{1}{\mathcal{L}_{3n}} \sum_{j:|\mathcal{V}_j|>1} \sum_{i \in \mathcal{V}_j} \exp(c_i^n) [\|\Delta \mathbf{A}_{ij}^n\| + \|\Delta \boldsymbol{\eta}_{ij}^n\|] \rightarrow 0, \quad (71)$$

as $n \rightarrow \infty$. Taking the summation of three limits in equations (65), (68) and (71), we deduce that $1 = \mathcal{L}_{3n} / \mathcal{L}_{3n} \rightarrow 0$ as $n \rightarrow \infty$, which is a contradiction. Thus, at least one among ratios of the forms $S_{n,j,\alpha_1,\alpha_2} / \mathcal{L}_{3n}$ and $T_{n,j,\ell} / \mathcal{L}_{3n}$ goes to zero as n tends to infinity.

Step 3 - Application of Fatou's lemma. In this step, we show that all the ratios $S_{n,j,\alpha_1,\alpha_2} / \mathcal{L}_{3n}$ and $T_{n,j,\ell} / \mathcal{L}_{3n}$ go to zero as $n \rightarrow \infty$, which contradicts to the conclusion in Step 2. In particular, by denoting m_n as the maximum of the absolute values of those ratios. From the result of Step 2, it follows that $1/m_n \not\rightarrow \infty$.

Recall from the hypothesis in equation (61) that $\|\tilde{f}_{G_n} - \tilde{f}_{G_*}\|_{L_2(\mu)} / \mathcal{L}_{3n} \rightarrow 0$ as $n \rightarrow \infty$, which indicates that $\|\tilde{f}_{G_n} - \tilde{f}_{G_*}\|_{L^1(\mu)} / \mathcal{L}_{3n} \rightarrow 0$. Therefore, by applying the Fatou's lemma, we get that

$$0 = \lim_{n \rightarrow \infty} \frac{\|\tilde{f}_{G_n} - \tilde{f}_{G_*}\|_{L^1(\mu)}}{m_n \mathcal{L}_{3n}} \geq \int \liminf_{n \rightarrow \infty} \frac{|\tilde{f}_{G_n}(\mathbf{x}) - \tilde{f}_{G_*}(\mathbf{x})|}{m_n \mathcal{L}_{3n}} d\mu(\mathbf{x}) \geq 0.$$

This result implies that $\frac{1}{m_n \mathcal{L}_{3n}} \cdot [\tilde{f}_{G_n}(\mathbf{x}) - \tilde{f}_{G_*}(\mathbf{x})] \rightarrow 0$ as $n \rightarrow \infty$ for μ -almost surely x . Looking at the formulation of $Q_n(\mathbf{x})$ in equation (63), since the term $\left[\sum_{j=1}^{N^*} \exp(\mathbf{x}^\top \mathbf{A}_j^* \mathbf{x} + c_j^*) \right]$ is bounded, we deduce that the term $\frac{1}{m_n \mathcal{L}_{3n}} \cdot Q_n(\mathbf{x}) \rightarrow 0$ for μ -almost surely x .

Let us denote

$$\frac{S_{n,j,\alpha_1,\alpha_2}}{m_n \mathcal{L}_{3n}} \rightarrow \phi_{j,\alpha_1,\alpha_2}, \quad \frac{T_{n,j,\ell}}{m_n \mathcal{L}_{3n}} \rightarrow \varphi_{j,\ell},$$

with a note that at least one among them is non-zero. Then, from the decomposition of $Q_n(\mathbf{x})$ in equation (64), we have

$$\begin{aligned} & \sum_{j=1}^{N^*} \sum_{|\alpha_1|+|\alpha_2|=0}^{1+\mathbf{1}_{\{|\mathcal{V}_j|>1\}}} \phi_{j,\alpha_1,\alpha_2} \cdot \frac{\partial^{|\alpha_1|} E}{\partial A^{\alpha_1}}(\mathbf{x}; \mathbf{A}_j^*) \frac{\partial^{|\alpha_2|} h}{\partial \boldsymbol{\eta}^{\alpha_2}}(\mathbf{x}; \boldsymbol{\eta}_j^*), \\ & - \sum_{j=1}^{N^*} \sum_{|\ell|=0}^{1+\mathbf{1}_{\{|\mathcal{V}_j|>1\}}} \varphi_{j,\ell} \cdot \frac{\partial^{|\ell|} E}{\partial A^\ell}(\mathbf{x}; \mathbf{A}_j^*) \tilde{f}_{G_*}(\mathbf{x}) = 0, \end{aligned}$$

for μ -almost surely x . It is worth noting that the term $\frac{\partial^{|\alpha_1|} E}{\partial A^{\alpha_1}}(\mathbf{x}; \mathbf{A}_j^*) \frac{\partial^{|\alpha_2|} h}{\partial \boldsymbol{\eta}^{\alpha_2}}(\mathbf{x}; \boldsymbol{\eta}_j^*)$ can be explicitly expressed as

- When $|\alpha_1| = 0, |\alpha_2| = 0$: $\exp(\mathbf{x}^\top \mathbf{A}_j^* \mathbf{x}) h(\mathbf{x}; \boldsymbol{\eta}_j^*)$;
- When $|\alpha_1| = 1, |\alpha_2| = 0$: $x^{(u)} x^{(v)} \exp(\mathbf{x}^\top \mathbf{A}_j^* \mathbf{x}) h(\mathbf{x}; \boldsymbol{\eta}_j^*)$;
- When $|\alpha_1| = 0, |\alpha_2| = 1$: $\exp(\mathbf{x}^\top \mathbf{A}_j^* \mathbf{x}) \frac{\partial h}{\partial \boldsymbol{\eta}^{(w)}}(\mathbf{x}; \boldsymbol{\eta}_j^*)$;
- When $|\alpha_1| = 1, |\alpha_2| = 1$: $x^{(u)} x^{(v)} \exp(\mathbf{x}^\top \mathbf{A}_j^* \mathbf{x}) \frac{\partial h}{\partial \boldsymbol{\eta}^{(w)}}$;
- When $|\alpha_1| = 2, |\alpha_2| = 0$: $x^{(u)} x^{(v)} x^{(u')} x^{(v')} \exp(\mathbf{x}^\top \mathbf{A}_j^* \mathbf{x}) h(\mathbf{x}; \boldsymbol{\eta}_j^*)$;
- When $|\alpha_1| = 0, |\alpha_2| = 2$: $\exp(\mathbf{x}^\top \mathbf{A}_j^* \mathbf{x}) \frac{\partial^2 h}{\partial \boldsymbol{\eta}^{(w)} \partial \boldsymbol{\eta}^{(w')}}(\mathbf{x}; \boldsymbol{\eta}_j^*)$.

Recall that the expert function h satisfies the condition in Definition B.2, i.e. the set

$$\left\{ x^\nu \cdot \frac{\partial^{|\gamma|} h}{\partial \boldsymbol{\eta}^\gamma}(\mathbf{x}; \boldsymbol{\eta}_j^*) : j \in [N^*], \frac{|\nu|}{2} \in \{0, 1, 2\}, 0 \leq |\gamma| \leq 2 - \frac{|\nu|}{2} \right\}$$

is linearly independent for μ -almost surely x . Therefore, we obtain that $\phi_{j,\alpha_1,\alpha_2} = \varphi_{j,\ell} = 0$ for all $j \in [N^*], 0 \leq |\alpha_1| + |\alpha_2|, |\ell| \leq 1 + \mathbf{1}_{\{|\mathcal{V}_j|>1\}}$. This result turns out to contradict the fact that at least one among them is different from zero. Hence, we achieve the inequality in equation (60).

E Additional Results

In this appendix, we study the identifiability of the MoE models with the quadratic polynomial gate and the quadratic monomial gate in that order.

Proposition E.1. *If $f_G(x) = f_{G_*}(x)$ holds true for almost every \mathbf{x} , then we get that $G \equiv G'$.*

Proof of Proposition E.1. Since $f_G(x) = f_{G_*}(x)$ for almost every \mathbf{x} , we have

$$\begin{aligned} & \sum_{i=1}^N \text{Softmax}\left(\mathbf{x}^\top \mathbf{A}_i \mathbf{x} + (\mathbf{b}_i)^\top \mathbf{x} + c_i\right) \cdot h(\mathbf{x}, \boldsymbol{\eta}_i) \\ &= \sum_{i=1}^{N_*} \text{Softmax}\left(\mathbf{x}^\top \mathbf{A}_i^* \mathbf{x} + (\mathbf{b}_i^*)^\top \mathbf{x} + c_i^*\right) \cdot h(\mathbf{x}, \boldsymbol{\eta}_i^*). \end{aligned} \quad (72)$$

Note that since the expert function $h(\cdot, \boldsymbol{\eta})$ satisfies the conditions in Definition 3.2, then given an arbitrary $N' \in \mathbb{N}$, then the set $\{h(\mathbf{x}, \boldsymbol{\eta}'_i) : i \in [N']\}$, where $\boldsymbol{\eta}'_1, \dots, \boldsymbol{\eta}'_{N'}$ are distinct vectors, is linearly independent for almost every \mathbf{x} . If $N \neq N_*$, then there exists some $i \in [N]$ such that $\boldsymbol{\eta}_i \neq \boldsymbol{\eta}_j^*$ for any $j \in [N_*]$. This implies that $\text{Softmax}\left(\mathbf{x}^\top \mathbf{A}_i \mathbf{x} + (\mathbf{b}_i)^\top \mathbf{x} + c_i\right) = 0$, which is a contradiction. Thus, we must have that $N = N_*$. As a result, we get that

$$\left\{ \text{Softmax}\left(\mathbf{x}^\top \mathbf{A}_i \mathbf{x} + (\mathbf{b}_i)^\top \mathbf{x} + c_i\right) : i \in [N] \right\} = \left\{ \text{Softmax}\left(\mathbf{x}^\top \mathbf{A}_i^* \mathbf{x} + (\mathbf{b}_i^*)^\top \mathbf{x} + c_i^*\right) : i \in [N_*] \right\},$$

for almost every \mathbf{x} . WLOG, we may assume that

$$\text{Softmax}\left(\mathbf{x}^\top \mathbf{A}_i \mathbf{x} + (\mathbf{b}_i)^\top \mathbf{x} + c_i\right) = \text{Softmax}\left(\mathbf{x}^\top \mathbf{A}_i^* \mathbf{x} + (\mathbf{b}_i^*)^\top \mathbf{x} + c_i^*\right), \quad (73)$$

for almost every \mathbf{x} for any $i \in [N_*]$. It is worth noting that the Softmax function is invariant to translations, then equation (73) indicates that $\mathbf{A}_i = \mathbf{A}_i^* + \mathbf{T}_2$, $\mathbf{b}_i = \mathbf{b}_i^* + \mathbf{t}_1$ and $c_i = c_i^* + t_0$ for some $\mathbf{T}_2 \in \mathbb{R}^{d \times d}$, $\mathbf{t}_1 \in \mathbb{R}^d$ and $t_0 \in \mathbb{R}$. However, from the assumptions $\mathbf{A}_k = \mathbf{A}_k^*$, $\mathbf{b}_k = \mathbf{b}_k^* = \mathbf{0}_d$ and $c_k = c_k^* = 0$, we deduce that $\mathbf{T}_2 = \mathbf{0}_{d \times d}$, $\mathbf{t}_1 = \mathbf{0}_d$ and $t_0 = 0$. Consequently, we get that $\mathbf{A}_i = \mathbf{A}_i^*$, $\mathbf{b}_i = \mathbf{b}_i^*$ and $c_i = c_i^*$ for any $i \in [N_*]$. Then, equation (72) can be rewritten as

$$\sum_{i=1}^{N_*} \exp(c_i) \exp\left(\mathbf{x}^\top \mathbf{A}_i \mathbf{x} + (\mathbf{b}_i)^\top \mathbf{x}\right) h(\mathbf{x}, \boldsymbol{\eta}_i) = \sum_{i=1}^{N_*} \exp(c_i^*) \exp\left(\mathbf{x}^\top \mathbf{A}_i^* \mathbf{x} + (\mathbf{b}_i^*)^\top \mathbf{x}\right) h(\mathbf{x}, \boldsymbol{\eta}_i^*), \quad (74)$$

for almost every \mathbf{x} . Next, we denote P_1, P_2, \dots, P_M as a partition of the index set $[N_*]$, where $M \leq N_*$, such that $\exp(c_i) = \exp(c_{i'}^*)$ for any $i, i' \in P_j$ and $j \in [N_*]$. On the other hand, when i and i' do not belong to the same set P_j , we let $\exp(c_i) \neq \exp(c_{i'}^*)$. Thus, we can reformulate equation (74) as

$$\begin{aligned} & \sum_{j=1}^M \sum_{i \in P_j} \exp(c_i) \exp\left(\mathbf{x}^\top \mathbf{A}_i \mathbf{x} + (\mathbf{b}_i)^\top \mathbf{x}\right) h(\mathbf{x}, \boldsymbol{\eta}_i) \\ &= \sum_{j=1}^M \sum_{i \in P_j} \exp(c_i^*) \exp\left(\mathbf{x}^\top \mathbf{A}_i^* \mathbf{x} + (\mathbf{b}_i^*)^\top \mathbf{x}\right) h(\mathbf{x}, \boldsymbol{\eta}_i^*), \end{aligned}$$

for almost every \mathbf{x} . Recall that $\mathbf{A}_i = \mathbf{A}_i^*$, $\mathbf{b}_i = \mathbf{b}_i^*$ and $c_i = c_i^*$ for any $i \in [N_*]$, then the above equation implies that

$$\{\boldsymbol{\eta}_i : i \in P_j\} \equiv \{\boldsymbol{\eta}_i^* : i \in P_j\},$$

for almost every \mathbf{x} for any $j \in [m]$. As a consequence,

$$G = \sum_{j=1}^M \sum_{i \in P_j} \exp(c_i) \delta_{(\mathbf{A}_i, \mathbf{b}_i, \boldsymbol{\eta}_i)} = \sum_{j=1}^M \sum_{i \in P_j} \exp(c_i) \delta_{(\mathbf{A}_i^*, \mathbf{b}_i^*, \boldsymbol{\eta}_i^*)} = G_*$$

Hence, we reach the conclusion of this proposition. \square

Proposition E.2. *If $\tilde{f}_G(x) = \tilde{f}_{G_*}(x)$ holds true for almost every \mathbf{x} , then we get that $G \equiv G'$.*

The proof of Proposition E.2 can be done in a similar fashion to that of Proposition E.1.

F Experimental Details

F.1 Verification of Theoretical Results.

Model details. We now provide the details for the model parameters in model. The variance of Gaussian noise is specified as $\sigma^2 = 0.049$. The true parameters for the gating network, $(\mathbf{A}_i^*, \mathbf{b}_i^*, c_i^*) \in \mathbb{R}^{d \times d} \times \mathbb{R}^d \times \mathbb{R}$, are drawn independently of an isotropic Gaussian distribution with zero mean and variance $\sigma_r^2 = 0.01/d$ for $1 \leq i \leq 7$, and otherwise are set to zero. Similarly, the true parameters of the experts, $(\boldsymbol{\beta}_{1i}^*, \boldsymbol{\beta}_{0i}^*) \in \mathbb{R}^d \times \mathbb{R}$, are drawn independently of an isotropic Gaussian distribution with zero mean and variance $\sigma_e^2 = 1/d$ for all experts. These parameters remain unchanged for all experiments.

Training procedure. For each sample size n , spanning from 10^3 to 10^5 , we perform 20 experiments. In every experiment, the parameters initialization for the gate's and experts' parameters are adjusted to be near the true parameters, minimizing potential instabilities from the optimization process. Subsequently, we execute gradient descent for 10 epochs, employing a learning rate of $\eta = 0.1$ to fit a model to the synthetic data. All the numerical experiments are conducted on a MacBook Air equipped with an M1 chip CPU.

F.2 Performance of Active-Attention Mechanism.

F.2.1 Dataset Details

CIFAR-10 Dataset. CIFAR-10 [18] is an established computer-vision dataset used for object recognition. It consists of 60,000 32×32 color images containing one of 10 object classes ("plane", "car", "bird", "cat", "deer", "dog", "frog", "horse", "ship", "truck"), with 6000 images per class.

ImageNet Dataset. We use the ImageNet database from ILSVRC2012 [34] that contains $1.28M$ training images and $50K$ validation images, where the task is to classify images into 1,000 distinct categories, using a vast dataset of over 1.2 million training images and 150,000 validation and test images sourced from the ImageNet database.

WikiText-103 Dataset. WikiText-103 is a language modeling dataset that contains collection of tokens extracted from good and featured articles from Wikipedia, which is suitable for models that can leverage long-term dependencies. It contains around $268K$ words and its training set consists of about $28K$ articles with $103M$ tokens, this corresponds to text blocks of about 3600 words. The validation set and test sets consist of 60 articles with $218K$ and $246K$ tokens respectively.

Table 4: Statistics of time series benchmarks.

| Dataset | Weather | Traffic | Electricity | Illness | ETTh1 | ETTh2 | ETTm1 | ETTm2 |
|-----------|---------|---------|-------------|---------|-------|-------|-------|-------|
| Features | 21 | 862 | 321 | 7 | 7 | 7 | 7 | 7 |
| Timesteps | 52696 | 17544 | 26304 | 966 | 17420 | 17420 | 69680 | 69680 |

Multivariate Time Series Forecasting Datasets. The Weather dataset captures 21 meteorological indicators in Germany, such as humidity and air temperature. The Traffic dataset records road occupancy rates from various sensors on San Francisco freeways. The Electricity dataset provides hourly electricity consumption data for 321 customers. The Illness dataset tracks the number of patients and the influenza-like illness ratio on a weekly basis. The ETT (Electricity Transformer Temperature) datasets are collected from two different electric transformers, labeled 1 and 2, each containing data at two resolutions: 15 minutes (m) and 1 hour (h). This results in four ETT datasets: ETTm1, ETTm2, ETTh1, and ETTh2. Detailed statistics can be found in Table 4.

F.3 Model Details

ViT-Tiny is composed of 6 layers that integrate localized self-attention (LSA), feedforward networks (FFN), and PreNorm layer normalization, with 8 attention heads and 512 hidden dimensions. We use a patch size of 4 and GeLU as the activation function for the FFN. This model is employed in the CIFAR-10 experiment displayed in Figure 2 (a).

CaiT-Tiny consists of 6 layers of patch-to-patch attention and 2 layers of cross-attention between CLS tokens and patches, with 6 attention heads and 256 hidden dimensions. We use a patch size of 4 and GeLU as the activation function for the FFN. This model is utilized in the CIFAR-10 experiment shown in Figure 2 (a).

ViT-Base comprises 12 transformer layers of patch-to-patch attention with PreNorm layer normalization, it has 12 attention heads and 3072 hidden dimensions. We use a patch size of 16 and GeLU as the activation function for the FFN. This model is used for the ImageNet experiment depicted in Figure 2 (b).

CaiT-Medium consists of 24 layers of patch-to-patch attention and 2 layers of cross-attention between CLS tokens and patches, with 16 attention heads and 3072 hidden dimensions. We use a patch size of 16 and GeLU as the activation function for the FFN. This model is utilized in the ImageNet experiment shown in Figure 2 (b).

Language Models We used the small versions of language models developed by [35]. For both the Transformer and Performer models, the dimensions of the key, value, and query were set to 128, and the context length for training and evaluation was configured to 256. Each model was assigned 8 self-attention heads, with the feedforward network (FFN) having a hidden dimension of 2048. The number of attention layers was set to 16. These models are used for the WikiText-103 experiment depicted in Figure 2 (c).

<https://www.bgc-jena.mpg.de/wetter/>
<https://pems.dot.ca.gov/>
<https://archive.ics.uci.edu/ml/datasets/ElectricityLoadDiagrams20112014>
<https://gis.cdc.gov/grasp/fluvview/fluportaldashboard.html>
<https://github.com/zhouhaoyi/ETDataset>

Time Series Models We use the supervised PatchTST model with the default parameter configurations proposed in [27]. The look-back window is set to 336, with a patch length of 16 and a stride of 8. For the Illness dataset, the prediction length is 36, while for the rest of the datasets, it is set to 192. For the Transformer model, we use a standard self-attention transformer with an encoder-decoder architecture, consisting of 2 encoder layers and 1 decoder layer. The model uses 8 attention heads and a feed-forward network (FFN) hidden dimension of 2048.

F.4 Quadratic Gating vs. Linear Gating.

F.4.1 Dataset details.

FineWeb-Edu Dataset. FineWeb-Edu 10BT [29] is a large-scale dataset with 10 billion tokens curated from diverse educational sources like textbooks and academic publications, designed to enhance language models for educational tasks. Its high-quality filtering and deduplication processes make it ideal for training relatively small-scale language models.

F.4.2 Model details.

GPT2-MoE. We examined the MoE adaptation of the GPT-2 [31] transformer structure. Specifically, we substituted the FFN layers with an MoE layer consisting of 8 experts. To ensure a fair comparison between MoE models and the dense model, we set the hidden size of the FFN layer (d_{ff}) so that the active parameters during inference are roughly equivalent. We also set the quadratic gate rank to 32 to limit the number of additional gating parameters. Refer to Table 5 for comprehensive details on the parameter counts. Details on the hyperparameters related to the architecture and training process are provided in Table 6.

| Model | d_{ff} | Active Params. | Total Params. |
|----------------------|-----------------|------------------|------------------|
| GPT2-dense | 3072 | $\approx 124.4M$ | $\approx 124.4M$ |
| GPT2-MoE (Linear) | 1536 | $\approx 124.5M$ | $\approx 166.9M$ |
| GPT2-MoE (Quadratic) | 1536 | $\approx 126.8M$ | $\approx 169.3M$ |

Table 5: Number of parameters in models.

G Computational Overhead of Quadratic Gating

In this section, we analyze the computational and memory overhead introduced by incorporating quadratic gating. Consider an MoE layer with N two-layer MLP experts with hidden size of d_{ff} . Note that each expert has $2d \times d_{\text{ff}}$ parameters. The linear gating network has d parameters per expert while the introduction of quadratic terms in the gating network increases the parameter count to at most $d + d(d + 1)/2$ per expert. Therefore, in each MoE layer the ratio of additional gating parameters to the total number of parameters is $d/4d_{\text{ff}}$.

Parameter count overhead. Note that this parameter count overhead is not necessarily negligible; however, this can be effectively managed by using low-rank embeddings for second-order terms in the router. For example, in Mixtral 8x7B, $d_{\text{ff}} = 3.5 \times d$ which results in approximately 7% increase

| Parameter | Value |
|---------------------|------------------|
| block_size | 1024 |
| vocab_size | 50257 |
| n_layer | 12 |
| n_head | 12 |
| n_embedding | 768 |
| n_experts | 8 |
| quadratic_gate_rank | 32 |
| total_batch_size | 524288 |
| batch_size | 64 |
| Optimizer | AdamW |
| weight_decay | 0.1 |
| lr_scheduler | CosineAnealingLR |
| max_lr | 0.0006 |
| min_lr | 0.00006 |
| warmup_steps | 19073 |

Table 6: Hyperparameters values.

in MoE layer parameter count if we use quadratic gating. The total parameter count overhead is almost 2.1B, which is about 4% of total number of parameters (47B) or 16% of total number of active parameters (13B). In particular, assuming that the query and key linear embeddings in the Att-MoE framework are low-rank with rank $r \ll d$, the number of additional parameters per expert can be reduced to $(\frac{N+1}{N})(r \times d)$. Therefore, the ratio of additional gating parameters to the total number of parameters in the MoE layers can be as low as $(\frac{N+1}{N})(r/2d_{ff})$. For the Mixtral 8x7B example, assuming $r = 128$, the total parameter count overhead reduces to 150M parameters, which is only 0.3% of all parameters and 1.1% of the active parameters, making it relatively insignificant. Similarly, in our experiments with GPT2 level models, we used $r = 32$, which leads to roughly 2.3M additional total parameters which is 1.4% of the total parameters and 1.8% of active parameters.

Computational overhead. The number of FLOPs is usually considered proportional to the number of non-embedding parameters. In the case of the Mixtral 8x7B example, utilizing low-rank embeddings with $r = 128$ for both query and key vectors within the Att-MoE framework adds 150M parameters, resulting in just a 1% increase in the number of FLOPs.

Memory overhead. Since all parameters must be loaded into memory for inference or training, the memory usage of MoE models is proportional to their total number of parameters. For example, in the Mixtral 8x7B model, using low-rank embeddings with $r = 128$ in the Att-MoE framework, which leads to merely a 0.3% increase in memory overhead.

References

- [1] A. Agarap. Deep learning using rectified linear units (relu). *arXiv preprint arXiv:1803.08375*, 2018. (Cited on page 11.)
- [2] D. Bahdanau, K. Cho, and Y. Bengio. Neural machine translation by jointly learning to align and translate, 2016. (Cited on page 4.)
- [3] G. Blecher and S. Fine. Moeatt: A deep mixture of experts model using attention-based routing gate. In *2023 International Conference on Machine Learning and Applications (ICMLA)*, pages 1018–1024. IEEE, 2023. (Cited on page 5.)
- [4] Z. Chen, Y. Deng, Y. Wu, Q. Gu, and Y. Li. Towards understanding the mixture-of-experts layer in deep learning. In S. Koyejo, S. Mohamed, A. Agarwal, D. Belgrave, K. Cho, and A. Oh, editors, *Advances in Neural Information Processing Systems*, volume 35, pages 23049–23062. Curran Associates, Inc., 2022. (Cited on page 16.)
- [5] K. Choromanski, V. Likhoshesterov, D. Dohan, X. Song, A. Gane, T. Sarlos, P. Hawkins, J. Davis, A. Mohiuddin, L. Kaiser, et al. Rethinking attention with performers. *arXiv preprint arXiv:2009.14794*, 2020. (Cited on page 11.)
- [6] D. Dai, C. Deng, C. Zhao, R. Xu, H. Gao, D. Chen, J. Li, W. Zeng, X. Yu, Y. Wu, et al. Deepseekmoe: Towards ultimate expert specialization in mixture-of-experts language models. *arXiv preprint arXiv:2401.06066*, 2024. (Cited on page 2.)
- [7] A. Dosovitskiy. An image is worth 16x16 words: Transformers for image recognition at scale. *arXiv preprint arXiv:2010.11929*, 2020. (Cited on page 11.)
- [8] N. Du, Y. Huang, A. M. Dai, S. Tong, D. Lepikhin, Y. Xu, M. Krikun, Y. Zhou, A. Yu, O. Firat, B. Zoph, L. Fedus, M. Bosma, Z. Zhou, T. Wang, E. Wang, K. Webster, M. Pellat, K. Robinson, K. Meier-Hellstern, T. Duke, L. Dixon, K. Zhang, Q. Le, Y. Wu, Z. Chen, and C. Cui. Glam: Efficient scaling of language models with mixture-of-experts. In *ICML*, 2022. (Cited on page 1.)
- [9] S. Elfwing, E. Uchibe, and K. Doya. Sigmoid-weighted linear units for neural network function approximation in reinforcement learning. *Neural networks*, 107:3–11, 2018. (Cited on page 11.)
- [10] W. Fedus, B. Zoph, and N. Shazeer. Switch transformers: Scaling to trillion parameter models with simple and efficient sparsity. *Journal of Machine Learning Research*, 23:1–39, 2022. (Cited on pages 1 and 2.)
- [11] T. Gale, D. Narayanan, C. Young, and M. Zaharia. Megablocks: Efficient sparse training with mixture-of-experts. *Proceedings of Machine Learning and Systems*, 5, 2023. (Cited on page 1.)
- [12] X. Han, H. Nguyen, C. Harris, N. Ho, and S. Saria. Fusemoe: Mixture-of-experts transformers for fleximodal fusion. In *Advances in Neural Information Processing Systems*, 2024. (Cited on page 1.)
- [13] D. Hendrycks and K. Gimpel. Gaussian error linear units (gelus). *arXiv preprint arXiv:1606.08415*, 2016. (Cited on page 11.)

[14] N. Ho and X. Nguyen. Convergence rates of parameter estimation for some weakly identifiable finite mixtures. *Annals of Statistics*, 44:2726–2755, 2016. (Cited on page 7.)

[15] R. A. Jacobs, M. I. Jordan, S. J. Nowlan, and G. E. Hinton. Adaptive mixtures of local experts. *Neural Computation*, 3, 1991. (Cited on page 1.)

[16] A. Q. Jiang, A. Sablayrolles, A. Roux, A. Mensch, B. Savary, C. Bamford, D. S. Chaplot, D. de las Casas, E. B. Hanna, F. Bressand, G. Lengyel, G. Bour, G. Lample, L. R. Lavaud, L. Saulnier, M.-A. Lachaux, P. Stock, S. Subramanian, S. Yang, S. Antoniak, T. L. Scao, T. Gervet, T. Lavril, T. Wang, T. Lacroix, and W. E. Sayed. Mixtral of experts. *arxiv preprint arxiv 2401.04088*, 2024. (Cited on pages 1 and 2.)

[17] M. I. Jordan and R. A. Jacobs. Hierarchical mixtures of experts and the EM algorithm. *Neural Computation*, 6:181–214, 1994. (Cited on pages 1 and 4.)

[18] A. Krizhevsky, G. Hinton, et al. Learning multiple layers of features from tiny images. 2009. (Cited on pages 11 and 34.)

[19] D. Lepikhin, H. Lee, Y. Xu, D. Chen, O. Firat, Y. Huang, M. Krikun, N. Shazeer, and Z. Chen. GShard: Scaling Giant Models with Conditional Computation and Automatic Sharding. In *International Conference on Learning Representations*, 2021. (Cited on pages 1 and 2.)

[20] H. Liang, Z. Fan, R. Sarkar, Z. Jiang, T. Chen, K. Zou, Y. Cheng, C. Hao, and Z. Wang. M³ViT: Mixture-of-Experts Vision Transformer for Efficient Multi-task Learning with Model-Accelerator Co-design. In *NeurIPS*, 2022. (Cited on page 1.)

[21] X. Liao, H. Li, and L. Carin. Quadratically gated mixture of experts for incomplete data classification. In *Proceedings of the 24th International Conference on Machine learning*, pages 553–560, 2007. (Cited on pages 2 and 13.)

[22] T. Manole and N. Ho. Refined convergence rates for maximum likelihood estimation under finite mixture models. In *Proceedings of the 39th International Conference on Machine Learning*, volume 162 of *Proceedings of Machine Learning Research*, pages 14979–15006. PMLR, 17–23 Jul 2022. (Cited on page 8.)

[23] S. Merity, C. Xiong, J. Bradbury, and R. Socher. Pointer sentinel mixture models, 2016. (Cited on page 11.)

[24] B. Mustafa, C. Ruiz, J. Puigcerver, R. Jenatton, and N. Houlsby. Multimodal contrastive learning with limoe: the language-image mixture of experts. In *NeurIPS*, 2022. (Cited on page 1.)

[25] H. Nguyen, N. Ho, and A. Rinaldo. On least square estimation in softmax gating mixture of experts. In *Proceedings of the International Conference on Machine Learning*, 2024. (Cited on page 8.)

[26] H. Nguyen, T. Nguyen, and N. Ho. Demystifying softmax gating function in Gaussian mixture of experts. In *Advances in Neural Information Processing Systems*, 2023. (Cited on page 8.)

[27] Y. Nie, N. H. Nguyen, P. Sinthong, and J. Kalagnanam. A time series is worth 64 words: Long-term forecasting with transformers. In *International Conference on Learning Representations*, 2023. (Cited on pages 11 and 36.)

[28] C. Nwankpa, W. Ijomah, A. Gachagan, and S. Marshall. Activation functions: Comparison of trends in practice and research for deep learning. *arXiv preprint arXiv:1811.03378*, 2018. (Cited on page 11.)

[29] G. Penedo, H. Kydlíček, A. Lozhkov, M. Mitchell, C. Raffel, L. Von Werra, T. Wolf, et al. The fineweb datasets: Decanting the web for the finest text data at scale. *arXiv preprint arXiv:2406.17557*, 2024. (Cited on pages 12 and 36.)

[30] J. Puigcerver, C. Riquelme, B. Mustafa, and N. Houlsby. From sparse to soft mixtures of experts. In *The Twelfth International Conference on Learning Representations*, 2024. (Cited on page 1.)

[31] A. Radford, J. Wu, R. Child, D. Luan, D. Amodei, I. Sutskever, et al. Language models are unsupervised multitask learners. *OpenAI blog*, 1(8):9, 2019. (Cited on pages 12 and 36.)

[32] C. Riquelme, J. Puigcerver, B. Mustafa, M. Neumann, R. Jenatton, A. S. Pint, D. Keysers, and N. Houlsby. Scaling vision with sparse mixture of experts. In *Advances in Neural Information Processing Systems*, volume 34, pages 8583–8595. Curran Associates, Inc., 2021. (Cited on page 1.)

[33] C. Ruiz, J. Puigcerver, B. Mustafa, M. Neumann, R. Jenatton, A. Pinto, D. Keysers, and N. Houlsby. Scaling vision with sparse mixture of experts. In *NeurIPS*, 2021. (Cited on page 1.)

[34] O. Russakovsky, J. Deng, H. Su, J. Krause, S. Satheesh, S. Ma, Z. Huang, A. Karpathy, A. Khosla, M. Bernstein, et al. Imagenet large scale visual recognition challenge. *International journal of computer vision*, 115:211–252, 2015. (Cited on pages 11 and 34.)

[35] I. Schlag, K. Irie, and J. Schmidhuber. Linear transformers are secretly fast weight programmers. In *International Conference on Machine Learning*, pages 9355–9366. PMLR, 2021. (Cited on page 35.)

[36] N. Shazeer, A. Mirhoseini, K. Maziarz, A. Davis, Q. Le, G. Hinton, and J. Dean. Outrageously large neural networks: The sparsely-gated mixture-of-experts layer. In *In International Conference on Learning Representations*, 2017. (Cited on pages 1, 2, and 4.)

[37] H. Touvron, M. Cord, A. Sablayrolles, G. Synnaeve, and H. Jégou. Going deeper with image transformers. In *Proceedings of the IEEE/CVF international conference on computer vision*, pages 32–42, 2021. (Cited on page 11.)

[38] S. van de Geer. *Empirical processes in M-estimation*. Cambridge University Press, 2000. (Cited on pages 6 and 16.)

[39] A. Vaswani, N. Shazeer, N. Parmar, J. Uszkoreit, L. Jones, A. N. Gomez, Ł. Kaiser, and I. Polosukhin. Attention is all you need. *Advances in neural information processing systems*, 30, 2017. (Cited on pages 2, 4, and 11.)

[40] L. Xu, M. Jordan, and G. E. Hinton. An alternative model for mixtures of experts. *Advances in neural information processing systems*, 7, 1994. (Cited on page 13.)

[41] B. Yu. Assouad, Fano, and Le Cam. *Festschrift for Lucien Le Cam*, pages 423–435, 1997. (Cited on page 26.)

[42] Y. Zhou, N. Du, Y. Huang, D. Peng, C. Lan, D. Huang, S. Shakeri, D. So, A. Dai, Y. Lu, Z. Chen, Q. Le, C. Cui, J. Laudon, and J. Dean. Brainformers: Trading simplicity for efficiency. In *International Conference on Machine Learning*, pages 42531–42542. PMLR, 2023. (Cited on page 1.)